Iranian Journal of Electrical and Electronic Engineering 03 (2020) 371–392
Special Issue on Smart Grids

Iran University of Science and Technology

Iranian Journal of Electrical and Electronic Engineering

Journal Homepage: ijeee.iust.ac.ir

Research Paper

Stochastic Joint Optimal Distributed Generation Scheduling and Distribution Feeder Reconfiguration of Microgrids Considering Uncertainties Modeled by Copula-Based Method

M. Khajehvand*, A. Fakharian*(C.A.), and M. Sedighizadeh**

Abstract: Using distributed generations (DGs) with optimal scheduling and optimal distribution feeder reconfiguration (DFR) are two aspects that can improve efficiency as well as technical and economic features of microgrids (MGs). This work presents a stochastic copula scenario-based framework to jointly carry out optimal scheduling of DGs and DFR. This framework takes into account non-dispatchable and dispatchable DGs. In this paper, the dispatchable DG is a fuel cell unit and the non-dispatchable DGs with stochastic generation are wind turbines and photovoltaic cells. The uncertainties of wind turbine and photovoltaic generations, as well as electrical demand, are formulated by a copula-based method. The generation of scenarios is carried out by the scenario tree method and representative scenarios are nominated with scenario reduction techniques. To obtain a weighted solution among the various solutions made by several scenarios, the average stochastic output (ASO) index is used. The objective functions are minimization of the operational cost of the MG, minimization of active power loss, maximization of voltage stability index, and minimization of emissions. The best-compromised solution is then chosen by using the fuzzy technique. The capability of the proposed model is investigated on a 33-bus MG. The simulation results show the efficiency of the proposed model to optimize objective functions, while the constraints are satisfied.

Keywords: Copula-Based Method, Distribution Feeder Reconfiguration (DFR), Distributed Generation (DG), Microgrids (MGs), Scheduling, Uncertainty.

Nomenclature

Sets

N_{BR}	Set of branches.
$N_{DG_{ND}}$	Set of non-dispatchable DGs.
$N_{DG_{D}}$	Set of dispatchable DGs.
N_{bus}	Set of buses.
S	Set of scenarios.
N_p	Set of populations.
D	Set of decision variables.
K	Set of iterations.

Variables

$P_{loss}(s)$	Active power loss and *s*-th scenario [kW].
$I(k.s)$	Current in *k*-th branch and *s*-th scenario [A].
$VSI_r(s)$	Voltage stability index for *r*-th bus and *s*-th scenario [pu].
$V_z(s)$	Voltage for *z*-th bus and *s*-th scenario [pu].
$P_{zr}(s)$	Active power between *z*-th and *r*-th buses and *s*-th scenario [pu].
$Q_{zr}(s)$	Reactive power between *z*-th and *r*-th buses and *s*-th scenario [pu].
$C_{grid}(s)$	Cost of energy exchanged with upstream grid and *s*-th scenario [$].

Iranian Journal of Electrical and Electronic Engineering, 2020.
Paper first received 30 September 2019, revised 02 January 2020, and accepted 07 January 2020.
* The authors are with the Department of Electrical, Biomedical, and Mechatronics Engineering, Qazvin Branch, Islamic Azad University, Qazvin, Iran.
E-mails: khajehvand222@yahoo.com and ahmad.fakharian@qiau.ac.ir.
** The author is with the Faculty of Electrical Engineering, Shahid Beheshti University, Evin, Tehran, Iran
E-mail: m_sedighi@sbu.ac.ir.
Corresponding Author: A. Fakharian.

$C_{DG_{ND}}(i.s)$	Cost of active power generated by i-th non-dispatchable DG [$].
$C_{DG_D}(j.s)$	Cost of active power generated by j-th dispatchable DG and s-th scenario [$].
$P_{grid}(s)$	Active power exchanged with upstream grid [kW].
$P_{DG_{ND}}(i.s)$	Active power generated by i-th non-dispatchable DG and s-th scenario [kW].
$P_{DG_D}(j.s)$	Active power generated by j-th dispatchable DG and s-th scenario [kW].
$f_i(s)$	Value of i-th objective function and s-th scenario.
f_i^{min}	Nadir value for i-th objective function.
f_i^{max}	Ideal value for i-th objective function.
$a_i(s)$	Fuzzy membership for i-th objective function and s-th scenario.
$PG(i.s)$	Generated active power in i-th bus and s-th scenario [pu].
$PD(i.s)$	Demanded active power in i-th bus and s-th scenario [pu].
$\|V(i.s)\|$	Magnitude of voltage in ith bus and s-th scenario [pu].
$\delta(i.s)$	Phase voltage in i-th bus and s-th scenario [pu].
$\|Y(i.j)\|$	Magnitude of admittance of between i-th and j-th bus [pu].
$\varphi(i.j.s)$	Phase of admittance of between i-th and j-th bus [pu].
$QG(i.s)$	Generated reactive power in i-th bus and s-th scenario [pu].
$QD(i.s)$	Demanded reactive power in i-th bus and s-th scenario [pu].
$\|I(i.j.s)\|$	Magnitude of current of between i-th and j-th bus and s-th scenario [pu].
$X_j^{(k.i)}$	j-th candidate solution for i-th particle in k-th iteration.
$V_j^{(k.i)}$	j-th element of velocity vector for i-th particle in k-th iteration.
$Gbest_j^{(k)}$	Global best position all of candidate solution found up to k-th iteration.
$Pbest_j^{(k.i)}$	Best previous experience for i-th particle in k-th iteration.
$\psi_r(X.Y)$	Rank correlation.
$G_X(X)$	Calmative distribution function (CDF) of X random variable.
$G_Y(Y)$	Calmative distribution function (CDF) of Y random variable.
$\mathrm{Cov}(G_X.G_Y)$	Covariance of G_X and G_Y.
$\sigma(G_X)$	Standard deviation of G_X.
$\sigma(G_Y)$	Standard deviation of G_Y.
Parameters	
$R(k)$	Resistance of k-th branch [Ω)].
R_{zr}	Resistance between z-th and r-th buses [pu].
X_{zr}	Reactance between z-th and r-th buses [pu].
$\rho_{grid}(t)$	Price of electricity in the upstream market at t-th hour [$/kW].
$a_{DG_{ND}}(i)$	Investment (fix) cost of i-th non-dispatchable DG [$].
$b_{DG_{ND}}(i)$	Variable cost of i-th non-dispatchable DG [$].
$a_{DG_D}(i)$	Investment (fix) cost of i-th dispatchable DG [$].
$b_{DG_D}(i)$	Variable cost of i-th non-dispatchable DG [$].
η_{ele}	Electrical efficiency of dispatchable DGs.
$Cost_{Capital}^{DG}$	Capital cost of DGs [$/kW].
$P_{Capacity}^{DG}$	Capacity of DGs [kW].
Gr	Annual rate of benefit.
$CF_{DG}(i)$	Capacity factor of i-th DG.
T_{Life}	Life time of DGs [year].
$Cost_{DG_D}^{O\&M}$	Cost of operation and maintenance of dispatchable DGs [$/kW].
$Cost_{DG_D}^{Fuel}$	Cost of fuel of dispatchable DG [$/kW].
$Cost_{DG_{ND}}^{O\&M}$	Cost of operation and maintenance of non-dispatchable DGs [$/kW].
ρ_{gas}	Price of natural gas in the upstream market [$/m^3].
β_{gas}	Rate of exchanging natural gas to electricity [m^3/kW].
$ER(j)$	Emission rate of j-th DG [kg/kW].
ER_{grid}	Emission rate of grid [kg/kW].
I_{ij}^{max}	Permitted current of feeder or cable between i-th and j-th bus [pu].
V_{min}	Maximum allowable voltage in each bus [pu].
V_{max}	Minimum allowable voltage in each bus [pu].
$P_{DG_D}^{min}(i)$	Minimum allowable active power generated by ith dispatchable DG [kW].
$P_{DG_D}^{max}(i)$	Maximum allowable active power generated by i-th dispatchable DG [kW].
$r_1.r_2$	Random number from the Gaussian distribution.
$c_1.c_2$	Inertia coefficients.
si	Solar irradiance [kW/m^2].
$f_b(si)$	Beta PDF of si.
α_s	Parameters of the Beta PDF.
β_s	Parameters of the Beta PDF.
μ_s	Mean of forecasted solar irradiance [kW/m^2].
σ_s	Standard deviation of forecasted solar irradiance [kW/m$^{2]}$.
η_{pv}	Efficiency of PV module.
S_{pv}	Area of PV module [m^2].
P_{rated}	Rated output power of WT [kW].
v_r	Rated wind speed [m/s].
v	Wind speed [m/s].
v_{ct}	Cut-in wind speed [m/s].
v_{co}	Cut-out wind speed [m/s].
μ_d	Mean of forecasted electrical demand [kW].

σ_d	Standard deviation of forecasted electrical demand [kW].
z	A vector of random variables between zero and one.
$\rho(s)$	Probability of scenario s.

Abbreviations

ASO	Average stochastic output.
CDF	Cumulative distribution function.
DFR	Distribution feeder reconfiguration.
DG	Distributed generation.
FC	Fuel cell.
IMOPSO	Improved multi-objective particle swarm optimization.
MG	Microgrid.
MGO	Microgrid operator.
MOP	Multi-objective problem.
MOPSO	Multi-objective particle swarm optimization.
MGO	Microgrid operator.
MLP	Multi-layer perceptron.
O&M	Operation and maintenance.
PV	Photovoltaic.
PDF	Probability distribution function.
PSO	Particle swarm optimization.
SOP	Single objective problem.
VSI	Voltage stability index (VSI).
WT	Wind turbine.

ASO	Average stochastic output.
CDF	Cumulative distribution function.
DFR	Distribution feeder reconfiguration.
DG	Distributed generation.
FC	Fuel cell.
IMOPSO	Improved multi-objective particle swarm optimization.
MG	Microgrid.
MGO	Microgrid operator.
MOP	Multi-objective problem.
MOPSO	Multi-objective particle swarm optimization.
MGO	Microgrid operator.
MLP	Multi-layer perceptron.
O&M	Operation and maintenance.
PV	Photovoltaic.
PDF	Probability distribution function.
PSO	Particle swarm optimization.
SOP	Single objective problem.
VSI	Voltage stability index (VSI).
WT	Wind turbine.

1 Introduction

1.1 Motivation and Incitement

CURRENTLY, the DGs based on renewable energy resources such as WTs and PVs are attracting the attention of the MGO and even consumers due to the lack of need for fuel, lower operational cost, and less emission [1]. Moreover, they motivate small investors for contributing to the generation of electrical power. The DGs are mainly connected to distribution networks, including MGs. They have a wide range of capacities and technologies such as WTs, PVs, FCs, and etc. [2]. The optimal scheduling of DGs improves the key operational factors of MGs that are active power loss, operational cost, voltage stability and emissions [3, 4].

Distribution networks, including MGs, are normally operated in a radial topology due to the simplicity of the protection coordination and reducing the short-circuit level. The DFR is an operational task that changes the open/close status of sectionalizer and tie switches to enhance the quality of operation in the MGs. However, the MGs have numerous switching combinations, and finding the optimal combination in each hour can be a sophisticated optimization problem for MGO [3].

1.2 Literature Review

There are several researches dedicated to joint problem of optimal DFR and energy management MGs. In [3], a multi-objective fuzzy framework is presented for simultaneous optimal DFR and optimal scheduling of DGs in the distribution network. The proposed method consists of the objective functions of power losses, voltage stability, DG cost, and emissions. In [2], the optimal DFR and optimal scheduling of DGs are simultaneously performed by a multi-objective hybrid big bang big crunch (MOHBB-BC) algorithm. The objective functions are similar to [3], however, the uncertainty of electrical loads is modeled using the Triangular Fuzzy Number (TFN) technique. The important weakness of [2, 3] is to ignore the stochastic behavior of non-dispatchable DGs. In [5], a stochastic multi-objective model is proposed for the optimal DFR and planning of DGs to minimize MGO's costs without considering emission effects. In [6], a stochastic model for optimal planning of DGs and DFR is proposed to consider the upstream grid market. The stochastic behavior of electrical demand and WTs are modeled. However, the other stochastic generation, such as PV and non-dispatchable DGs are not addressed in this reference. In [7] a two-stage method for optimal energy management and DFR is proposed to consider non-dispatchable DGs in an MG. Yet, the uncertainties of electrical demands are not taken into consideration. In [8], a MOP for optimal energy management and DFR is proposed. The aim of optimization is the minimization of active power losses, annual operation costs, and emissions simultaneously. Nonetheless, the pattern of the variation in wind speed, solar irradiation, and electrical demand is considered as a deterministic time sequence. In [9], the optimal energy management and DFR are simultaneously performed by Hong's 2m point estimate method. The goals of optimization are to minimize operational costs as well as to improve the reliability and resiliency of the MGs considering the stochastic pattern of generation. In [10], an MOP based on optimal DFR and energy management is proposed for minimizing active power losses and phase unbalancing and improving the voltage profile. In [11], a joint stochastic problem for optimal DFR and energy management is proposed. Solving proposed MOP leads to the minimization of active power loss and number of switching operations as well as the maximization of the voltage stability margin. In [12], a stochastic MOP is proposed for the optimal DFR and energy management to maximize the DG owner's profit and minimize the distribution company's costs. In [1], a MOP is proposed based on optimal DFR in parallel with energy management for minimizing active power loss, annual operation costs that are installation, maintenance, and active power loss costs and emissions. In [13], an MOP is proposed to optimize DFR and energy management with two goals that are to minimize active power loss and to improve the voltage stability index. The proposed MOP is solved by the Cuckoo search algorithm. In [14], an energy management methodology is presented considering DFR. The objective functions are minimization of the total cost, including investment cost of DG, operation and management cost of DG, the fuel cost of DG, and demand-side management cost. In [15], the dedicated search teaching-learning based optimization (DSTLBO) algorithm is proposed for simultaneous energy management considering DFR to maximize energy loss reduction subject to improve voltage profiles. In [16], a planning method is proposed to maximize the profits of DFR and energy management. It considers numerous objective functions that are investment, operation and maintenance costs and environmental effects. In [17], the metaheuristic harmony search algorithm combined with sensitivity analysis is presented to perform optimal DFR and energy management simultaneously. In [18], an efficient hybrid heuristic search algorithm based on the harmony search algorithm and particle artificial bee colony algorithm is proposed for simultaneous DFR along with optimal energy management of MG, including DGs. In [19], a combination of a fuzzy approach and bacterial foraging optimization (BFO) is developed to solve the simultaneous DFR, and energy management in an MG. In [20], a fuzzy MOP including DFR, and energy management is simultaneously solved by non-dominated sorting genetic algorithm (NSGA-II). The objective functions are minimization of voltage deviation, maximization of voltage stability index, lower amount of pollutant and lower cost. The studies that are performed for simultaneous DFR and scheduling of microgrid can be classified from different perspectives, including the type of formulation, the selected objective functions, the model for uncertainty in the formulation, and the solution methodology. Table 1 lists the recent references regarding the above-mentioned criteria.

1.3 Contribution and Paper Organization

Table 1 shows the differences between the proposed model and other works. Indeed, the present work extends the model proposed by authors in [2], and [3]

Table 1 Recent research works addressing DFR and scheduling in microgrids.

Reference No.	Type of formulation	Objective function	Uncertainty		Solution method		Reactive power control	DER
			Demand	Generation	Mathematical	Heuristic		
[1]	Deterministic	Real power loss, annual operation costs and emissions	-	-	-	Strength Pareto Evolutionary Algorithm 2 (SPEA2)	-	WT, PV
[2]	Deterministic	Operation cost, power loss, emissions, and voltage stability	-	-	-	HBB-BC	-	WT, PV, MT, FC
[3]	Stochastic	Operation cost, power loss, emissions, and voltage stability	✓	-	-	Pareto based HBB-BC	-	WT, PV, MT, FC
[5]	Stochastic	Operation cost, reliability, power loss, and number of switching	-	✓	GAMS	-	-	WT, PV, BM, MT, SH, FC, GT, Electric Vehicle
[6]	Stochastic	Benefit of MGO	✓	✓	-	PSO	-	WT, MT, BESS
[7]	Deterministic	Cost of energy	-	-	-	PSO	-	WT, PV
[9]	Stochastic	Operation cost, resiliency, and reliability	✓	✓	-	EMA	-	WT, PV, CHP, BESS
[10]	Deterministic	Phase unbalancing, power loss, voltage profile, and operation cost	-	-	-	Bacterial Foraging with Spiral Dynamic algorithm	-	General form of DER
[11]	Stochastic	Power loss, voltage stability, and number of switching	✓	-	-	Knee point driven evolutionary algorithm	-	SH
[12]	Stochastic	DG owner's profit and the distribution company's costs	✓	✓	GAMS	-	-	WT
[13]	Deterministic	Real power loss and voltage stability	-	-	-	CSA	-	General form of DER
[14]	Deterministic	Operation cost and demand side cost	-	-	-	Differential evolution algorithm	-	General form of DER
[15]	Deterministic	energy loss and voltage profile	-	-	-	DSTLBO	✓	General form of DER
[16]	Deterministic	Costs of line upgrades, energy losses, switching operations, DG capital, operation and maintenance costs and emissions	-	-	GAMS	-	-	General form of DER
[17]	Deterministic	Real power loss and voltage profile	-	-	-	Harmony Search Algorithm (HSA)	-	General form of DER
[18]	Deterministic	Real power loss and voltage profile	-	-	-	integrating PSO and ABC algorithm with HSA	✓	General form of DER
[19]	Deterministic	Real power loss and voltage profile	-	-	-	bacterial foraging optimization (BFO)	✓	General form of DER
[20]	Deterministic	Operation cost, reliability, and power quality	-	-	-	NSGA-II	✓	General form of DER
Current paper	Stochastic	Operation cost, power loss, emissions, and voltage stability	✓	✓	-	IMOPSO	✓	WT, PV, FC

with considering the uncertainties of generation and demand. Besides, the uncertainties of WT and PV generation, and electrical demand are modeled by the copula-based method which has received less attention in the similar work. The scenario tree is used to generate scenarios and representative scenarios are nominated with scenario reduction techniques. Another innovation is to use the ASO index for obtaining a weighted solution among the various solutions made by numerous scenarios. The objective functions of the proposed MOP are to minimize the operational cost, to minimize active power loss, to maximize VSI, and to minimize emissions considering different constraints. A Pareto based MOP is derived, and by using the fuzzy decision-maker and a novel algorithm, named IMOPSO, the best-compromised solution is chosen.

The main contributions provided by this paper as follows:

- Extending [2], and [3] with considering the uncertainties of generations and demand.
- Using the copula-based method for modeling the stochastic pattern of wind speed, solar irradiance, and electrical demand.
- Using a stochastic optimization based on IMOPSO algorithm.
- Using an ASO index to obtain a weighted solution among the numerous solutions made by several scenarios.

The rest of this paper is organized as follows. In Section 2, the proposed problem formulation are elucidated. The uncertainty modeling is elucidated in Section 3. The proposed IMPSO is explained in Section 4. The implementation of the proposed algorithm on proposed MOP is described in Section 5. The simulation results are presented in Section 5 to assess the benefits of this work. Finally, the conclusions are delineated in Section 6.

2 Problem Formulation

This section involves the formulation of objective functions and constraints.

2.1 Objective Functions

2.1.1 Minimization of Active Power Losses

Minimization of active power losses is one of the key issues in the operation of MGs that can be calculated as follows [21]:

$$\min f_1(s) = P_{loss} = \sum_{k \in N_{BR}} R(k) \times \left| I(k.s) \right|^2 \quad \forall s \in S \tag{1}$$

2.1.2 Maximization of VSI

From the voltage stability point of view, the VSI should be maximized in order to have a stable MG. For a typical radial feeder with two end buses of *z* and *r*, the VSI for bus *r* is expressed as follows [2, 22]:

$$\begin{aligned} VSI_r(s) = {} & \left[V_z(s)\right]^4 - 4 \times \left[P_{zr}(s) \times X_{zr} - Q_{zr}(s) \times R_{zr}\right]^2 \\ & - 4 \times \left[V_z(s)\right]^2 \times \left[P_{zr}(s) \times R_{zr} - Q_{zr}(s) \times X_{zr}\right] \\ & \forall s \in S,\ \forall r.z \in N_{bus} \text{ for } z \neq r \end{aligned} \tag{2}$$

The bus, which has the lowest VSI would be the one which is the most sensitive one to voltage collapse. This means that the critical buses have the most deviation of VSI from unity. To maximize the weakest VSI, the second objective function is defined as follows [2, 22]:

$$\min f_2(s) = \max_r^t \left\{ 1 - VSI_r(s) \right\} \quad \forall r \in N_{bus} \tag{3}$$

2.1.3 Minimization of Total Operational Cost

In this paper, it is assumed the MGO is owner of the DGs, therefore, the total operational cost of MG deals with the cost of energy exchanged with upstream grid, and cost of active power generated by DGs. The total operational cost is written in the following [23]:

$$\begin{aligned} \min f_3(s) = {} & C_{grid}(s) + \sum_{i \in N_{DG_{ND}}} C_{DG_{ND}}(i.s) \\ & + \sum_{j \in N_{DG_D}} C_{DG_D}(j.s) \quad \forall s \in S \end{aligned} \tag{4}$$

The cost of energy exchanged with upstream grid is written as follows [23]:

$$C_{grid}(s) = P_{grid}(s) \times \rho_{grid} \quad \forall s \in S \tag{5}$$

The cost of energy active power generated by DGs consists of two components that are the fix or investment costs (cost of equipment, infrastructure, commissioning, and etc.) and variable costs (cost of O&M and fuel costs). The cost of energy generated by DGs can be formulated as follows [24]:

For non-dispatchable DGs (PVs, and WTs):

$$C_{DG_{ND}}(i.s) = a_{DG_{ND}}(i) + b_{DG_{ND}}(i) \times P_{DG_{ND}}(i.s) \quad \forall s \in S,\ \forall i \in N_{DG_{ND}} \tag{6}$$

For dispatchable DGs (FCs):

$$C_{DG_D}(j.s) = a_{DG_D}(j) + b_{DG_D}(j) \times P_{DG_D}(j.s) \quad \forall t \in T,\ \forall s \in S,\ \forall j \in N_{DG_D} \tag{7}$$

where

$$a_{DG_{ND}}(i) = a_{DG_D}(j) = \frac{Cost_{Capital}^{DG} \times P_{Capacity}^{DG} \times Gr}{T_{Life} \times 365 \times 24 \times CF_{DG}(i)} \quad \forall i \in N_{DG_{ND}}.\forall j \in N_{DG_D} \tag{8}$$

$$\begin{cases} b_{DG_D}(j) = Cost_{DG_D}^{O\&M} + Cost_{DG_D}^{Fuel} \\ b_{DG_{ND}}(j) = Cost_{DG_{ND}}^{O\&M} & ,\forall i \in N_{DG_{ND}},\ \forall j \in N_{DG_D} \\ Cost_{DG_D}^{Fuel} = \beta_{gas} \times \rho_{gas} \end{cases} \tag{9}$$

2.1.4 Minimization of Total Emissions

The total emissions are concerned with the emissions generated by the upstream grid and FCs for generating electrical energy. The total emission is formulated as follows:

$$\min f_4(s) = P_{grid}(s) \times LF \times ER_{grid} \times 8760 + \left[\sum_{j \in N_{DG_D}} \left(\frac{P_{DG_D}(j,s)}{\eta_{ele}}\right) \times CF_{DG}(j) \times ER(j) \right] \times 8760 \quad \forall s \in S \tag{10}$$

2.2 Constraints

The proposed MOP subject to the following constraints:

2.2.1 Power Flow Equations

Active and reactive power balance at each bus of MG should be satisfied as follows [21]:

$$PG(i,s) - PD(i,s) = \sum_{j \in N_{bus}} |V(i,s)| \times |V(j,s)| \times |Y(i,j)| \times \cos\left(\delta(i,s) - \delta(j,s) - \varphi(i,j,s)\right) \quad \forall s \in S, \forall i \in N_{bus} \text{ for } i \neq j \tag{11}$$

$$QG(i,s) - QD(i,s) = \sum_{j \in N_{bus}} |V(i,s)| \times |V(j,s)| \times |Y(i,j)| \times \sin\left(\delta(i,s) - \delta(j,s) - \varphi(i,j,s)\right) \quad \forall s \in S, \forall i \in N_{bus} \text{ for } i \neq j \tag{12}$$

2.2.2 Network Radiality and Connectivity

One of the most important tasks in DFR is preservation of network radiality and connectivity [25]. In this paper, with the implementation of graph rules [26], the network radiality and connectivity is guaranteed.

2.2.3 Branch Current Limit

To be sure that the current of cables and feeders is not excessive from their rating, the following constraint should be taken into account [2]:

$$|I(i,j,s)| \leq I_{ij}^{max} \quad \forall s \in S, \forall i,j \in N_{bus} \text{ for } i \neq j \tag{13}$$

2.2.4 Bus Voltage Permissible Range

The voltage in each bus should meet the allowable range as follows [2]:

$$V_{min} \leq |V(i,s)| \leq V_{max} \quad \forall s \in S, \forall i \in N_{bus} \tag{14}$$

2.2.5 Dispatchable DGs Generation Limits

The output active power generated by dispatchable DGs should satisfy the following limit [2, 27]:

$$P_{DG_D}^{\min}(i) \leq P_{DG_D}(i,s) \leq P_{DG_D}^{\max}(i) \quad \forall s \in S, \forall i \in N_{DG_D} \tag{15}$$

2.2.6 DGs Penetration Level

The limit total power generated by DG units should be kept at a certain level so that the distribution network remains under control from special technical aspects. This level is specified as follows:

$$\sum_{i \in N_{DG_D}} P_{DG_D}(i,s) + \sum_{j \in N_{DG_{ND}}} P_{DG_{ND}}(j,s) \leq \pi \times \sum_{k \in N_{bus}} PD(k,s) \tag{16}$$

where π is the maximum penetration level of DGs.

3 Uncertainty Modeling

It is worthwhile to note that the different random variables are stochastically dependent on each other [28]. For instance, the forecasted and actual solar irradiance are significantly correlated together. Consequently, if the solar generation is precisely forecasted, then the actual solar generation is accurately planned. This statement can be expanded to other stochastic variables namely, wind speed, and electrical demand.

3.1 Calculation of Stochastic Correlation

The severity of correlation between the stochastic variables can be formulated as follows [28]:

$$\psi_r(X,Y) = \psi\left(G_X(X), G_Y(Y)\right) = \frac{Cov\left(G_X, G_Y\right)}{\sigma(G_X) \times \sigma(G_Y)} \tag{17}$$

It is seen that rank correlation factor ψ_r belongs to interval [0,1] and the random variable is transformed by this factor to uniform random space. When the rank correlation is one, the dependency between the random variables is high. On the contrary, if this factor is zero, thus the correlation is weak.

3.2 Copula Function

To formulate the multivariate distribution functions, one of the useful mathematical functions is copula function, which couples the several one-dimensional functions [29]. The coupling mechanism is carried out through to transform the uniform distribution of random variables in multivariate distribution space [29]. The details of copula function can be found in [28, 30].

It is assumed that *X* and *Y* are two random variables whose CDFs are G_X and G_Y, respectively. The copula *C* can be formulated to link their distribution function as follows [28]:

$$G_{XY}(X,Y) = C\left(G_X(X), G_Y(Y)\right) \tag{18}$$

If $G_X(X) = w$ and $G_Y(Y) = z$, where w and z are the realization of the uniform random variables *W* and *Z*, respectively. Therefore, (21) is rewritten as follows [28]:

$$C_{(W|Z)}(w,z)=G(X,Y)=G\left(G_X^{-1}(w),G_Y^{-1}(z)\right) \tag{19}$$

where $C(W|Z)$ is the conditional distribution of $(W|Z)$ and G^{-1} is the inverse of a univariate distribution function.

3.3 Solar Irradiance Modeling and PV Generation Output

The probability distribution of solar irradiance is usually fitted by a bimodal distribution that can be modeled as a linear combination of two unimodal distributions. For this purpose, the Beta PDF is used for each unimodal (Fig. 1) that can be obtained as follows [31, 32]:

$$f_b(si)=\begin{cases}\dfrac{\Gamma(\alpha_s+\beta_s)}{\Gamma(\alpha_s)\Gamma(\beta_s)}\times si^{(\alpha_s-1)}\times(1-si)^{(\beta_s-1)} & 0\le Si\le 1,\ \alpha_s\ge 0,\ \beta_s\ge 0\\ 0 & \text{otherwise}\end{cases} \tag{20}$$

$$\beta_s=(1-\mu_s)\times\left(\frac{\mu_s\times(1+\mu_s)}{\sigma_s^2}-1\right) \tag{21}$$

$$\alpha_s=\frac{\mu_s\times\beta_s}{(1-\mu_s)} \tag{22}$$

The mean and standard deviation of wind speed are forecasted by historical data, which are gathered from the adjacent meteorology station [32, 33].

The solar irradiance, area, and efficiency of the PV modules determine the output power of the PV unit. Consequently, after the Beta PDF is produced, the output power of the PV unit for the different states is computed as follows [31, 32]:

$$P_{pv}(si)=\eta^{pv}.S^{pv}.si \tag{23}$$

3.4 Wind Speed Modeling and WT Generation Output

The stochastic behavior of wind speed is commonly modeled by Weibull PDF which needs two parameters for modeling. These parameters are the scale factor and shape factor which show by *a* and *b*, respectively. In this paper, these parameters are considered as $a = v_{mean}/0.9$ and $b = 2$. It is assumed that the WT is at a

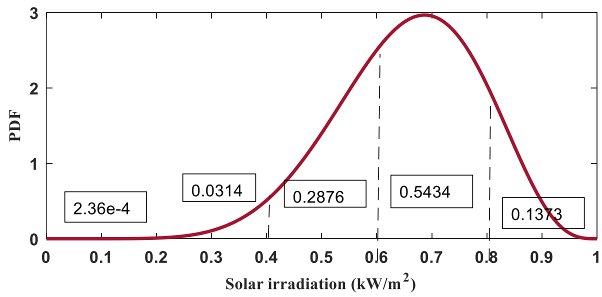

Fig. 1 Beta PDF for solar irradiation and its associated probability.

site where forecasted mean wind speed (v_{mean}) is known. The Weibull PDF used in this paper is specified by [32, 33]:

$$f_w(v)=ba^{-b}v^{b-1}e^{-\left(\frac{x}{a}\right)^b} \tag{24}$$

The output power of the WT is written as follows [32, 34]:

$$P_w(v)=\begin{cases}0 & 0\le v\le v_{ct}\\ P_{rated}\times\dfrac{(v-v_{ct})}{(v-v_{ct})} & v_{ct}\le v\le v_r\\ P_{rated} & v_r\le v\le v_{co}\\ 0 & v_{co}\le v\end{cases} \tag{25}$$

Fig. 2 displays the Weibull PDF for wind speed.

3.5 Electrical Demand Modeling

The uncertainty of forecasting electricity demand is regularly demonstrated by a Normal PDF which is given by [32, 35]:

$$f_d(l)=\frac{1}{\sigma_d\times\sqrt{2\pi}}\times e^{\frac{-(l-\mu_d)^2}{2\sigma_d^2}} \tag{26}$$
$$l=z\times\sigma_d+\mu_d$$

The Normal PDF for electrical demand is shown in Fig. 3.

3.6 State Selection

To consider the stochastic behavior of the output

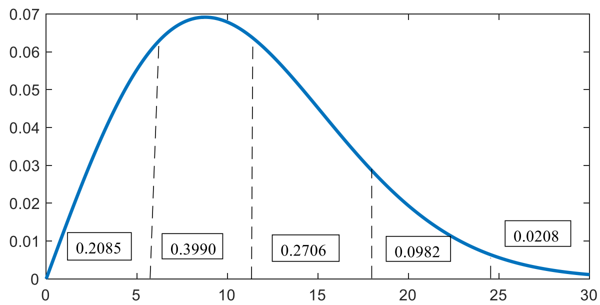

Fig. 2 Weibull PDF for wind speed and its associated probability.

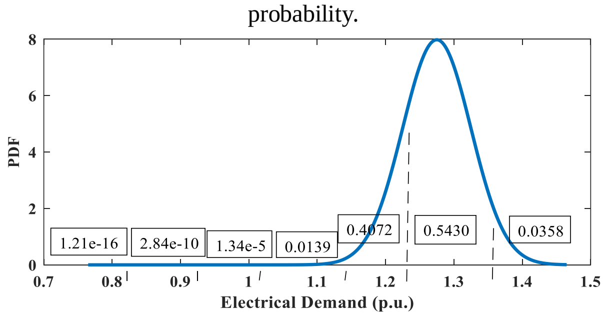

Fig. 3 Normal PDF for electrical demand and its associated probability.

power of PV, WT, and electrical demand in the proposed model, the continuous PDFs are divided into states (periods). In this paper, the number of states is assumed to be 5 for solar irradiance, 5 for wind speed, and 7 for electrical demand.

The probability of solar irradiance, wind speed, and electrical demand for each state is considered as follows [32, 36]:

$$P_s\{G_y\} = \int_{S_{y1}}^{S_{y2}} f_b(si)\,dsi \tag{27}$$

$$P_v\{G_w\} = \int_{V_{w1}}^{V_{w2}} f_w(v)\,dv \tag{28}$$

$$P_d\{G_L\} = \int_{d_{L1}}^{d_{L2}} f_d(l)\,dl \tag{29}$$

where $P_s\{G_Y\}$, $P_v\{G_W\}$, and $P_d\{G_L\}$ are the probability of the solar irradiance, wind speed, and electrical demand in states y, w, and L, respectively; s_{y1} and s_{y2} represent the solar irradiance limits of state y; v_{w1} and v_{w2} are the wind speed limits of state w; d_{L1} and d_{L2} are the load limits of state L; $f_b(si)$, $f_w(v)$, and $f_d(l)$ represent the probabilities for different states of PV unit, WT, and electrical demand, respectively.

3.7 Scenario Reduction Techniques

In this paper, the PV generation, WT generation, and electrical demand, including 5, 5, and 7 states, respectively. Regarding the scenario tree generation, 5×5×7=175 operating states should be studied. It is clear that a better modeling of the uncertainty deals with a higher number of scenarios while it needs a higher computational burden. Therefore, to well approximate stochastic behavior of MG, a suitable scenario reduction strategy should be applied to the model [37].

3.8 Automatic Clustering for Selecting Scenarios Using Genetic Algorithm

To minimize the intracluster spread, the K-means algorithm is one of the best alternatives that uses an iterative algorithm for clustering [38]. However, it has shortages that are dependent on the initial condition and the number of clusters specified by the user. This work clusters a dataset as an optimization problem that is solved by the genetic algorithm.

In this paper, a well-evaluated validity index named Davies-Bouldin (DB) is used for the automatic clustering algorithm [39]. In this index, the ratio between sums of within-cluster scatter to between cluster separations is calculated. The index uses both cluster and their corresponding sample mean. To begin, within i-th cluster distance and the distance between i-th and j-th clusters are denoted as follows [38, 39]:

$$S_{i.q} = \left[\frac{1}{N_i}\sum_{\bar{X}\in C_i}\left|\bar{X}-\overline{m_i}\right|^q\right]^{1/q} \qquad q \ge 1 \tag{30}$$

$$d_{ij.t} = \left[\sum_{p=1}^{d}\left|m_{i.p}-m_{j.p}\right|^t\right]^{1/t} = \overline{m_i}-\overline{m_j}_t \qquad t \ge 1 \tag{31}$$

where $S_{i.q}$ and $d_{ij.t}$ are within i-th cluster distance and the distance between i-th and j-th clusters, respectively; $\bar{m}_i$ is the i-th cluster center; N_i is the number of elements in the i-th cluster C_i; q (which is an integer) and t is arbitrary selected.

Next, $R_{i.qt}$ is given as [38, 39]:

$$R_{i.qt} = \max\left\{\frac{S_{i.q}+S_{j.q}}{d_{ij.t}}\right\} \qquad j \in k,\ j \ne i \tag{32}$$

Finally, the DB validity index is calculated as follows [38, 39]:

$$DB(K) = \frac{1}{K}\sum_{i=1}^{K} R_{i.qt} \tag{33}$$

The smallest $DB(K)$ validity index takes into account as an objective function that is solved by the genetic algorithm. After solving the optimization problem, at first, the specific number of centroids is selected and next, these selected centroids are allocated to the nearest scenario from the main scenario set and update the centroids. Then a redistribution of probabilities is performed. It comprises adding the probabilities of those scenarios which have not been finally selected to those recently updated centroids in every cluster. Thus, the reduced scenario set is provided by the final selected scenarios with associated probabilities.

ASO is a parameter indicating the average probable weighted output of a specified variable in the selected scenarios and it can be calculated as follows [40]:

$$ASO = \frac{\sum_{s\in S} PO(s)\times PVAR(s)}{\sum_{s\in S} PVAR(s)} \tag{34}$$

where $PO(s)$ represents the probable outcome of specific variable in the s-th selected scenario and $PVAR(s)$ shows the occurrence probability of that variable in the s-th selected scenario.

4 Improved Multi-Objective Particle Swarm Optimization (IMOPSO) Algorithm

In this paper, with the changes made to existing MOPSO optimization algorithms, a hybrid multi-objective algorithm with an appropriate accuracy and high-speed responsiveness known as IMOPSO is obtained; consequently, at first, the original PSO is briefly expressed and then presented algorithm is completely introduced.

4.1 Original PSO

The PSO algorithm is a set-based optimization algorithm that is inspired by the natural behavior of birds looking for food. Each solution of the problem is actually a bird in the search space known as particle. The algorithm is initialized with a random particle set. Each particle flies at a velocity across the multi-dimensional search space that its velocity and position are constantly improved by (35)-(36) with respect to the best previous position (*Pbest*) and the best global position (*Gbest*) [24].

$$V_j^{(k+1,i)} = \omega^{(k+1)} \times V_j^{(k,i)} + c_1 \times r_1 \times \left(Pbest_j^{(k,i)} - X_j^{(k,i)}\right) + c_2 \times r_2 \times \left(Gbest_j^{(k)} - X_j^{(k,i)}\right) \quad \forall j \in D, i \in N_p, \forall k \in K \tag{35}$$

$$X_j^{(k+1,i)} = X_j^{(k,i)} + V_j^{(k+1,i)} \quad \forall j \in D, i \in N_p, \forall k \in K \tag{36}$$

$$\omega^{(k+1)} = \omega^{max} - \frac{\omega^{max} - \omega^{min}}{t_{max}} \times k \qquad \forall k \in K \tag{37}$$

4.2 Multi-Objective PSO (MOPSO) and Improved MOPSO (IMOPSO) Algorithms

4.2.1 MOP

Solving the SOP results in finding an optimal solution. However, in the real world, the problem space is faced with several objective functions that often conflict together. To simultaneously optimize the several objective functions, a MOP should be formulated while the problem constraints are met. The MOP can be defined as follows [2, 22].

$$\min F = \left[f_1(x).f_2(x).\dots.f_n(x)\right]^T \tag{38}$$

$$\begin{cases} h_i(x) = 0 & i \in N_{eq} \\ g_i(x) \le 0 & i \in N_{ueq} \end{cases} \tag{39}$$

where x is the control variable for decision making, $f_i(x)$ is i-th objective function, and n is the number of objective functions. $h(x)$ and $g(x)$ show the equality and inequality constraints, respectively.

There are two general methods for solving the MOPs [41] including 1) using the aggregation operators for converting the MOP to SOP such as weighted sum and fuzzy aggregators. 2) using the non-dominated sorting methods and obtaining the Pareto sets solutions. This paper uses the second method which is explained as follows:

The optimal solution which is not improved in one of the objective functions unless worsens the performance of the solution in at least one of the rest is named Pareto optimal solution. Hence Y^* is named a Pareto optimal solution if finding a solution Y in Q is infeasible such that Y overcomes $Y^* \in Q$. $Q$is the set of all vectors (Y) which satisfies the constraints of the problem. By definition, if the following two conditions are met for the solution, Y_1 will dominate Y_2 [2]:

$$g_j(Y_1) \le g_j(Y_2) \qquad \forall j \in n \tag{40}$$

$$g_k(Y_1) < g_k(Y_2) \qquad \forall k \in n \tag{41}$$

4.2.2 IMOPSO Algorithm

One of the powerful algorithms used in MOPs is the MOPSO. This algorithm was first proposed by Coello in 2004 [42]. In the multi-objective problems, the word “best” does not have a specific meaning, because it looks for a set of solutions that are not dominated by any other solution [2].

In this paper, with improvements made to MOPSO algorithm, an improved MOPSO algorithm with a suitable accuracy and high response speed is obtained that converts it into a very powerful and efficient multi-objective algorithm known as Improved MOPSO (IMOPSO) to solve various optimization problems. The IMOPSO finds a set of the dominated solutions (Pareto solutions) during the process and stores them in a repository. For many MOPs, the number of Pareto optimal solutions might be high and perhaps unlimited. Therefore, in this paper for improving MOPSO, a crowding distance operator is used to control the size of the repository and its most diversity (spread). Therefore, after the end of the optimization process, a set of dominated solutions is achieved. One of the other improvements is to select the best compromise solution among Pareto solutions using fuzzy technique by combining objective function belongs to each solution based on priorities, finally a fuzzy fitness function belongs to each solution is obtained. In this paper, the “maximum geometric mean “ operator is used to determine the value of the fitness function, which seems more suitable than other operators [3]. Table 1 shows the steps of the proposed IMOPSO algorithm.

4.2.3 Choosing Best Personal Experience (Pbest)

In the proposed algorithm, a method based on the concept of superior classification is used for choosing new Pbests. Fig. 4 shows the principles of this method. With this approach, firstly, all Pbests and all solutions generated in the k-th iteration are combined, and a partial $2N$ population is formed, then, the concept of superior classification is applied.

Followed by implementing superior classification, the partial $2N$ population is divided into different fronts (classes). The first front is the most dominated front in the current population that dominates the second front. The next step is to choose the best-experienced location for each solution (new P_{best}), which is randomly selected from the upper part of the first front. Finally, N members should be selected based on the value of fitness. The selected N members play the role of Pbests in the next generation [23].

Table 1 The steps of implementation of IMOPSO algorithm.

1. Importing the input parameters of the algorithm;
2. Making the initial population and initial velocity of each particle;
3. Evaluating each particle based on objective functions;
4. Separating non-dominated members of the population based on the concept of dominance and their storage in the ¬external repository;
5. Selecting a leader among the ¬members of the repository for each particle and starts moving;
6. Generating a new solution and updating the best personal memory of each particle based on the concept of non-dominated sorting;
7. Selecting the dominated solutions and upgrading the repository;
8. Non-dominated members of the current population are added to the repository and the dominant members of the repository are removed;
9. Using a crowding distance operator to control the size of the repository and diversity;
10. If the termination conditions are not met, go back to step 5, otherwise, go to step 11;
11. Selecting the best-compromised solution among Pareto solutions.

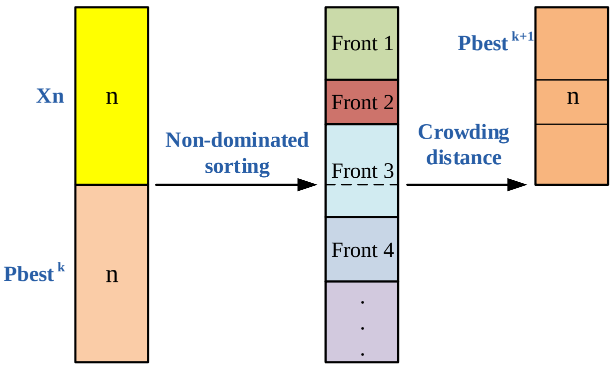

Fig. 4 Pbest selection.

4.2.4 Non-Dominated Sorting Method

In this method, for each member of the population, two parameters of n_p and S_p are defined. n_p or dominance counter refers the number of population members that are superior to p-th member, and S_p is a set of members to which the p-th member is superior. Since all these quantities have been calculated for all existing solutions in the population, these solutions should be classified in such a way that is based on n_p. This process continues in the same way for the next fronts until the solutions are eventually classified in different fronts.

4.2.5 Crowding Distance Operator

This operator acts based on concept of population density around a solution known as the "crowding distance". This operator provides the possibility of choosing more varied solutions from solutions located on a front. This distance is equal to the average distance between two solutions j-1 and j+1 that are located on the sides of j-th solution. Calculating the crowding distance attributed to each solution on a given front requires covering the following steps.

- ✓ Calculate the number of solutions located in n-th front and call it $L(|F_n|=L)$. For each I in this set, the initial value of swarm distance is assumed to be 0.
- ✓ Sort the existing solutions in the n-th front for each of the objective function $m \in M$ that M refers number of objective functions.
- ✓ Attribute a large swarm distance to the solutions located on the front border (initial and terminal solutions) for each objective function, m.

The crowding distance can be calculated as follows [43]:

$$Cd^m(I_j) = Cd^m(I_j) + \frac{f_m(I_{j+1}{}^m) - f_m(I_{j-1}{}^m)}{f_m^{max} + f_m^{min}}$$
$$\forall j \in n,\ m \in M \tag{42}$$

According to above, in the selection process of new Pbests among the $2N$ member set, the i-th solution is in priority compared to the j-th solution if at least one of the two below conditions is met:

I. i-th solution has a better ranking.
II. The ranking of both solutions is equal, but the crowding distance of i-th solution is greater than the j-th solution.

4.2.6 Selecting a Leader for Each Particle

Here, where the MOP is solved, there is no unique optimal solution, but there will be a repository of optimal solutions in the entire search space. Any solution in the Pareto repository can be a guide for population members. Here, instead of a unique Gbest, a different Gbest can be found from the repository for each member of the population.

In this paper, the concept of dominance is used to select Gbest for each member of the population; as Gbest is selected for X_n solution among the solutions from the repository that dominates X_n. If $A_{Xn} = \{\alpha \in A | \alpha < X_n\}$ shows a set of solutions in a repository that dominates X_n, then the relevant Gbest is randomly selected from this set, so that all members of this set have equal chances for being selected as guides. If X_n is not dominated by any member in the repository, if it is among the solutions of the repository, the set A_{Xn} will be empty, in which the relevant Gbest is randomly selected among all existing members in the repository [2]. The above expression can be formulated as follows:

$$Gbest_n = \begin{cases} a \in A & \text{with probability} \left|A\right|^{-1} \quad \text{if } X_n \in A \\ a \in A_{x_n} & \text{with probability} \left|A_{x_n}\right|^{-1} \quad \text{otherwise} \end{cases} \quad (43)$$

4.2.7 Selecting the Dominated Solutions and Upgrading the Repository

As noted earlier, the concept of dominance is used in order to find dominated solutions. In each iteration of algorithms, the new Pbest are extracted and become a candidate to be present in Pareto repository. The following four states might occur for a solution which candidates for adding to the repository:

1. If the repository of the dominated solutions is empty, then the new solution is added to the repository.
2. If the candidate's solution is not being dominated by any of the repository's solutions and if not dominated on any of it, which then goes to the repository.
3. If the candidate's solution dominates at least one of the archived solutions, then all dominant solutions are removed from the repository, and the new solution is added.
4. If the candidate's solution is dominated by one of the repository's solutions, then it is excluded. Since the capacity of the repository is limited, it is necessary to preserve the best and most varied solutions. Hence, the crowding distance operator is used here, and the solutions in low-density areas have a higher priority to remain in the repository to increase the variety of solutions in the repository.

4.2.8 Choosing the Best Compromised Solution

Solving the MOP by Pareto-based methods does not lead to a unique optimal solution that take the objective functions to the most optimal possible states, but in some studies, the methods are used to determine the best-compromised solution. Since objective functions have different dimensions, a method must be adopted for scaling. This paper uses a Fuzzy operator for scaling as follows [25, 26]:

$$a_i = \begin{cases} 1 & f_i < f_i^{\min} \\ \dfrac{f_i^{\max} - f_i}{f_i^{\max} - f_i^{\min}} & f_i^{\min} \le f_i \le f_i^{\max} \quad \forall i \in \{1,2,3,4\} \\ 0 & f_i \ge f_i^{\max} \end{cases} \quad (44)$$

To combine the scaled objective function, the "max geometric mean" operator is used as follows [25, 26]:

$$\mu = \left(\prod_{i \in M} \alpha_i \right)^{1/M} \quad (45)$$

Therefore, through this method, a value of fitness function μ is obtained for each solution of the problem that it is used to select the best-compromised solution.

Table 2 Parameters of the proposed algorithm for the case study.

Population size	ω_{min}	ω_{max}	C_1, C_2	Max iterations	$Trial^{Max}$
50	0.005	0.05	0.09, 0.1	100	35

The solution archived as an optimal Pareto solution that has the largest value of μ is proposed as the best-compromised solution.

5 Applying the IMOPSO Algorithm to Proposed MOP

For the proposed problem, decision variables include the status of open switches in each loop that are integer variables and output electrical power of dispatchable DGs, output electrical power of non-dispatchable DGs, and exchanged power with an upstream grid that are continuous variables. Consequently, the vector of decision variables can be as follows:

$$Y = \left[Tie(v), P_{grid}(t), P_{DG_{ND}}(i), P_{DG_D}(j)\right]$$
$$\forall v \in N_{Tie}, \forall i \in N_{DG_{ND}}, \forall j \in N_{DG_D} \quad (46)$$

Fig. 5 illustrates the flow chart of the implementation of IMOPSO algorithms to the proposed MOP. The termination criteria algorithm can be either when the maximum number of iterations is achieved or when the algorithms converge to an acceptable fitness value.

6 Simulation results

This section is partitioned through numerous subsections. Firstly, the two-dimensional PDFs stochastic parameters is simulated by copula-based method. These parameters are wind and solar power, and electrical demand. Next, the proposed MOP is solved by the proposed algorithm for a 32-bus MG. Finally, the optimal Pareto fronts and the best-compromised solution are derived. A trial and error process is used to tune the parameters of the proposed algorithm for the case study that is shown by Table 2. Due to the existence of random operators and for the sake of statistical analysis, the proposed algorithm is run several times. The maximum number of trials is displayed in Table 2. It should be noted that the simulations performed in this paper were implemented using the MATLAB (R2014b) software on a computer with Intel Core i7, 2.50GHz memory.

6.1 Modeling of Stochastic Parameters by Copula Function

Regarding Section 3, the copula function method needs the actual and predicted amounts of the stochastic parameters for time duration equal to one year. The real-time data that are solar irradiance, wind speed, and electrical demand is derived from our previous work [44]. An MLP neural network is used to obtain the

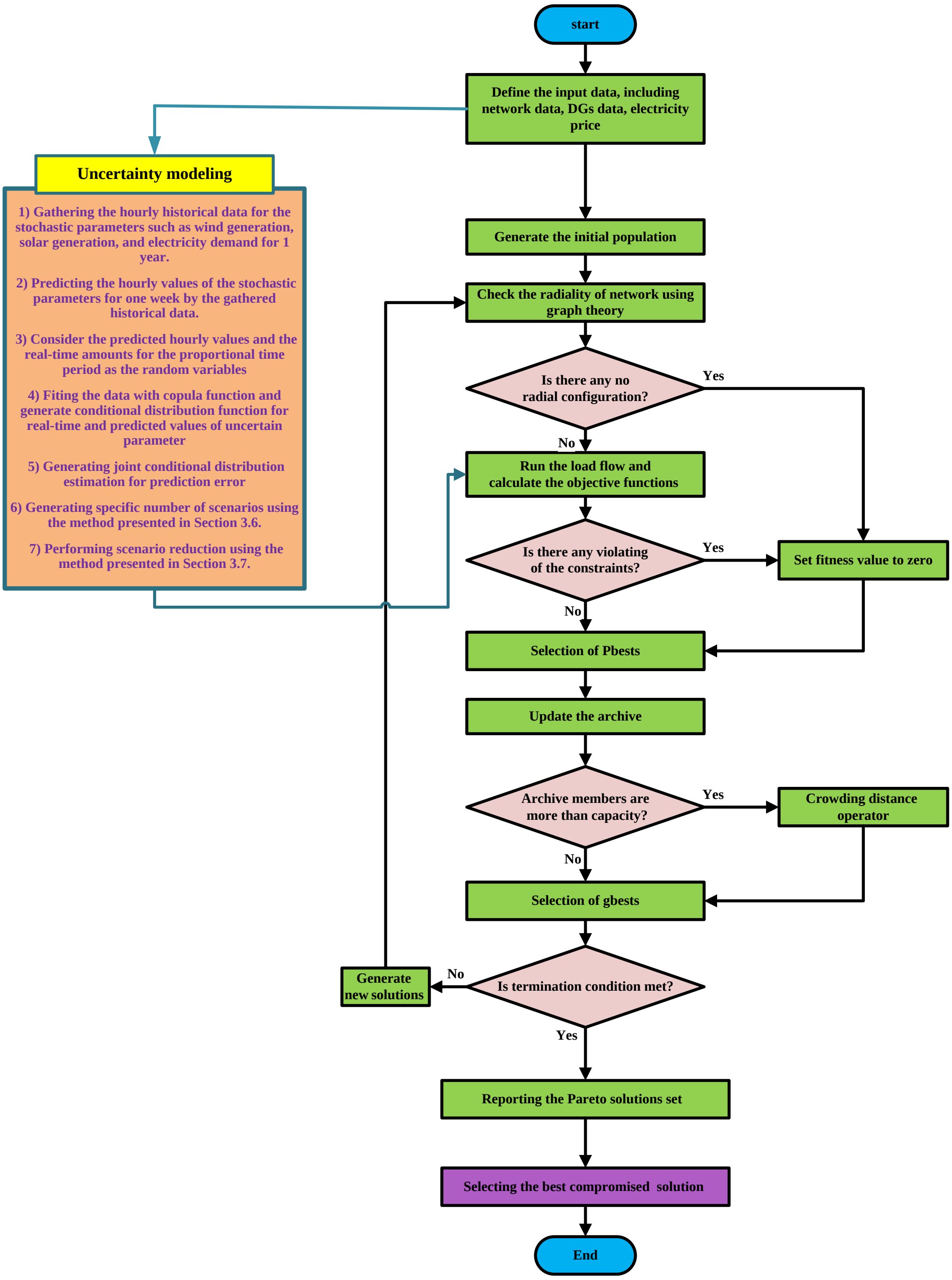

Fig. 5 Implementation of the IMOPSO algorithm on the proposed MOP problem.

predicted values of the stochastic parameters. Details of the implementation of the neural network have been described by [44]. Figs. 6-8 show the probabilistic relationship between the actual and the predicted data of solar power, wind power, and electrical demand.

To model multivariate PDFs, one of the most suitable copula functions is the Gaussian copula [45]. Therefore, in this paper, the Gaussian copula is used. The joint conditional distribution function of actual and predicted values of the stochastic parameters is displayed by Figs. 9-11

Figs. 9-11 confirm the PDFs assumed in Section 3 are very close to PDFs obtained from the actual stochastic data. It can be observed that the Fig. 9-11 approximately show the Beta, Weibull, and Normal PDF, respectively.

Firstly, the scenario generation is carried out by the algorithm proposed by Subsection 3.6. Then, the infeasible scenarios are reduced by the scenario reduction technique proposed by Subsection 3.8. Finally, the ASO index presented by the same

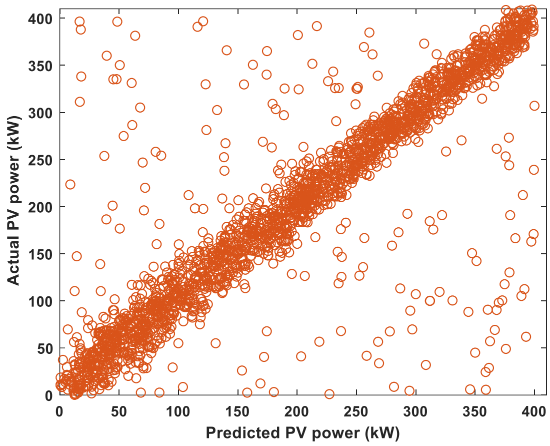

Fig. 6 The joint distribution of the actual and forecasted PV power.

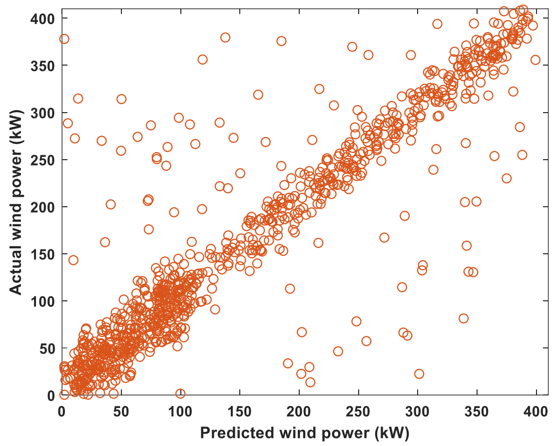

Fig. 7 The joint distribution of the actual and forecasted wind power.

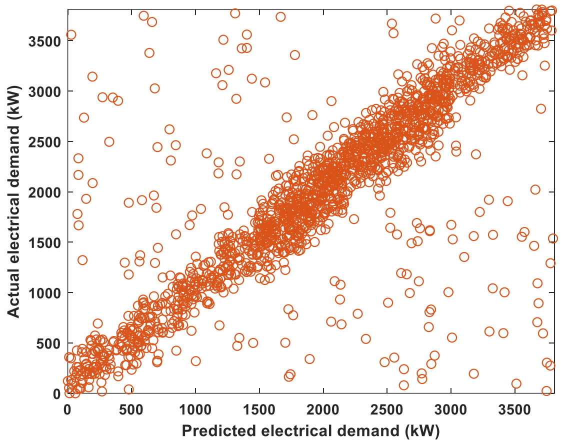

Fig. 8 The joint distribution of the actual and forecasted electrical demand.

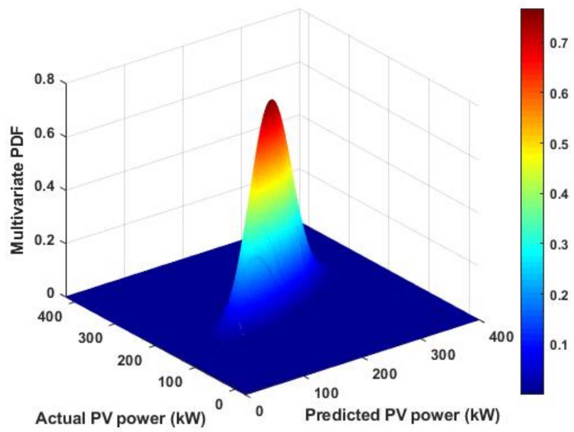

Fig. 9 The joint conditional distribution estimation of the actual and forecasted PV power.

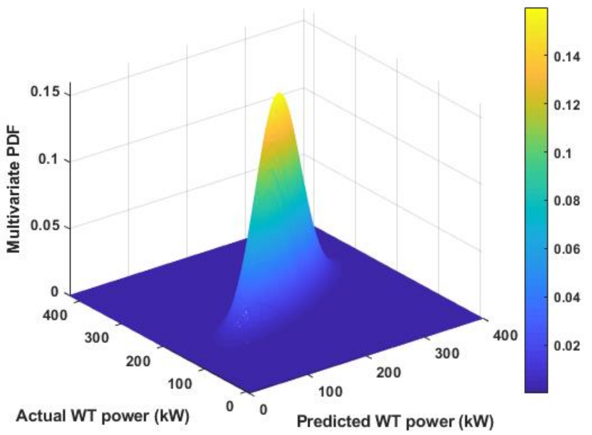

Fig. 10 The joint conditional distribution estimation of the actual and forecasted wind power.

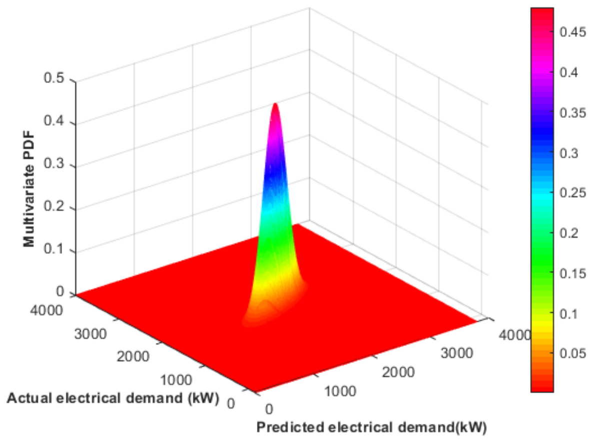

Fig. 11 The joint conditional distribution estimation of the actual and forecasted electrical demand.

subsection is applied to reduce the computational burden and to simplify the optimization process.

6.2 Thirty Two-Bus MG

To evaluate the IMOPSO algorithm to solve the proposed MOP, the simulation is performed on the case study of 33-bus MG [46]. The voltage level, the active and reactive power consumption of the understudy network is 12.66kV, 3715kW and 2300kVAr, respectively. The number of the tie (normally open) and sectionalizer (normally closed) switches in this radial distribution network is 5 and 32, respectively [2]. In Fig. 12, a single-line diagram of balance 32-bus MG is shown. Two combined energy systems, including PV, WT, and FC are installed on buses 4, and 14. In the basic configuration of the 33-bus distribution network without DFR and energy management (base case), the power loss, VSI, operational cost and emissions objective functions are 202.67kW, 0.6969, 219.38$/h and 22272 tons, respectively.

The details of the characteristics of combined energy system are represented in Table 3.

In this section, three case studies are taken into account to evaluate the proposed model. These case studies are as follows:

Case study 1: only optimal DFR without considering the combined energy systems.

Case study 2: only optimal energy scheduling the combined energy systems without DFR.

Case study 3: optimal energy scheduling the combined energy systems and DFR simultaneously.

6.2.1 Case Study 1

Table 4 lists the results of optimal DFR and values of the four objective functions as a set of Pareto optimal solutions. In this table, the optimal values of each objective function are colored. In this case study, the electrical demand and power losses are supplied by the upstream maim grid. Regarding Table 4, it is seen that solution numbers 14, 23, 25, and 28 have the best values for objective functions, including power loss, VSI, operation cost, and emission, respectively. It can be observed that the IMPSO cannot find a global optimum solution, while it obtains a set of the Pareto solutions which all of them are suitable for MGO. The selection

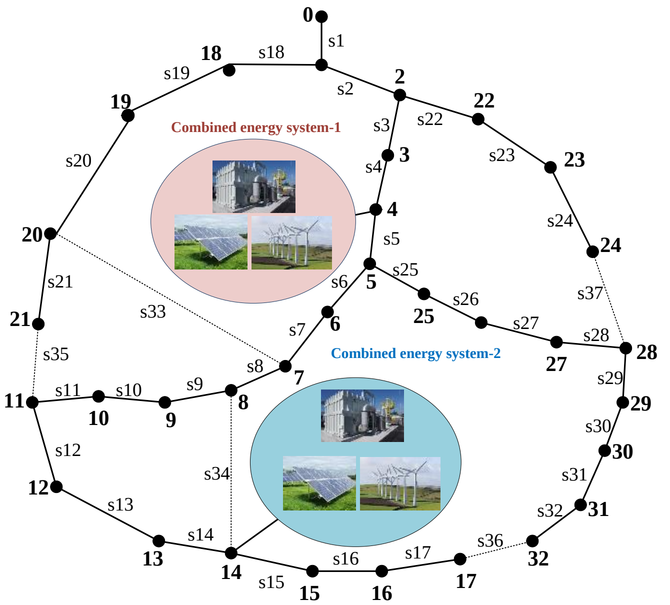

Fig. 12 The 33-bus MG.

Table 3 Data of combined energy system.

FC [3]		PV [32]		WT [32]	
Parameter	Value	Parameter	Value	Parameter	Value
$P_{DG_D}^{min}$	0	$Cost_{Capital}^{DG}$	6675	$Cost_{Capital}^{DG}$	1500
$P_{DG_D}^{max}$	400	$P_{Capacity}^{DG}$	400	$P_{Capacity}^{DG}$	400
$Cost_{Capital}^{DG}$	3674	Gr	0.136	Gr	0.136
$P_{Capacity}^{DG}$	400	CF_{DG}	0.25	CF_{DG}	0.2
Gr	0.136	T_{Life}	20	T_{Life}	20
CF_{DG}	0.2	$Cost_{DG_D}^{O\&M}$	0.05	$Cost_{DG_D}^{O\&M}$	0.05
T_{Life}	10	η^{pv}	18.6	P_{rated}	400
$Cost_{DG_D}^{O\&M}$	0.0039	S^{pv}	40	v_r	12
ER	14.447			v_{co}	25
Grid [3]				v_{ct}	3.5
V_{min}	0.90	* Units of quantities have been expressed in nomenclature.			
V_{max}	1.05				
ER_{grid}	27.34				

of the final solution depends on the preferences of the MGO. Nonetheless, the fuzzy technique presented by Subsection 4.2 is used for deriving the best-compromised solution. In this case study, this solution that is solution number 28 is bolded in Table 4. Fig. 13 shows the 3D plots of the objective functions.

Fig. 13 shows the optimal Pareto solution by star sign. Regarding the preferences of the MGO for optimizing a special objective function, the arrow sign shows the best solutions. Fig. 13 (a) displays the three objective functions such as power loss, operation cost, and emission which are plotted versus each other, and the VSI is not taken into account. It is seen that the optimal solution with coordinates (132.752kW (power loss), 220.084$/h (operation cost), and 22.14×10^3 ton (emission)) has the best solution for power loss objective functions, although it is not appropriate for the other objective functions. The other optimal solution with coordinates (133.02kW (power loss), 211.27$/h (operation cost), and 20.71×10^3 ton (emission)) is suitable for MGO whose priority is to minimize emissions. Also, if the preference of MGO is to reduce the operational cost, it is satisfied with the other optimal solution presented in Fig. 13 (a). Figs. 13 (b)-(d) illustrate that the best solution for VSI objective is 0.7969 (solution number 23), while this optimal solution has no suitable solutions for the other objectives that are 162.455kW (power loss), 226.258$/h (cost) and 24.823×$10^3$ ton (emission), respectively. The simulation results delineate that the goals of the proposed MOP are contradictory, so that an enhancement in one of them deteriorates the others. The red circles in Fig. 13 show the best-compromised solution, i.e. the solution number 28 in Table 3. It has coordinates (134.197 kW (power loss), 203.124$/h (operation cost), 20.723×10^3 tons (emission), 0.7736 (VSI)) that represents an appropriate compromise among the objectives.

6.2.2 Case Study 2

Table 5 represents the results of the optimal generation scheduling of the combined energy systems. This case study does not consider the DFR, therefore the statue of tie switches is like in the base case of 33-bus MG (Fig. 12). In this case study, the electrical demand and power losses are provided by the combined energy systems and the upstream main grid. The best solution for power loss, VSI, operation cost, and emission are related to solution number 25, 30, 28, and 1, respectively. However, the best-compromised solution obtained by the fuzzy decision maker corresponds to solution number 1. As regards Table 5, the FC-based generation units have a tendency to decrease the output power due to high emission rate. However, the PV and WT generation units in the combined energy system number 2 have tended to increase the power generation to the maximum capacity limit. This is due to the fact that renewable generation units have the low emission rate and operational cost compared to FC units and upstream generation units. Fig. 14 illustrates the 3D plots of the objective functions.

Similar to the previous case study, Fig. 14 (a)-(d)

Table 4 Set of the Pareto solutions (case study 1).

Solution number	Power losses [kW]	VSI	Cost [$/h]	Emission [tons]	Open switches in the best solution
1	133.197	0.7730	210.294	20.8036	7, 10, 14, 37, 31
2	134.082	0.7736	212.171	21.0379	7, 11, 14, 37, 31
3	157.427	0.7814	214.048	22.1775	6, 10, 14, 37, 34
4	132.952	0.7657	217.488	20.8238	7, 10, 13, 37, 31
5	157.617	0.7829	213.280	21.9049	6, 10, 14, 37, 34
6	155.348	0.7803	222.276	22.8813	7, 10, 14, 37, 34
7	132.977	0.7685	218.181	21.1688	7, 9, 13, 37, 31
8	134.748	0.7753	211.894	21.3043	7, 9, 14, 37, 31
9	162.138	0.7959	225.981	24.5476	6, 10, 14, 37, 34
10	135.758	0.7796	216.820	23.5373	6, 9, 14, 37, 31
11	158.563	0.7865	221.508	22.3223	6, 10, 14, 37, 34
12	158.841	0.7880	224.859	24.0471	6, 9, 14, 37, 34
13	159.227	0.7891	222.201	22.7766	6, 10, 14, 37, 34
14	132.752	0.7725	220.084	22.1405	7, 9, 13, 37, 31
15	160.907	0.7935	225.451	24.3751	6, 10, 14, 37, 34
16	135.398	0.7791	215.523	23.2632	6, 9, 14, 37, 31
17	156.684	0.7823	226.497	24.6800	7, 11, 14, 37, 34
18	132.904	0.7703	218.899	21.5153	7, 9, 13, 37, 31
19	159.631	0.7900	222.755	22.9644	6, 10, 14, 37, 34
20	135.275	0.7779	222.024	23.0568	6, 9, 14, 37, 31
21	160.534	0.7915	224.632	23.5620	6, 10, 14, 37, 34
22	135.590	0.7792	223.486	23.4495	6, 9, 14, 37, 31
23	162.544	0.7969	226.258	24.8232	6, 10, 14, 37, 34
24	155.686	0.7764	221.810	22.6226	7, 8, 14, 37, 34
25	133.021	0.7676	211.276	20.7149	7, 10, 13, 37, 31
26	160.657	0.7927	224.506	23.854	6, 10, 14, 37, 34
27	132.945	0.7712	219.353	21.6647	7, 9, 13, 37, 31
28	**134.197**	**0.7736**	**203.124**	**20.7237**	**7, 9, 14, 37, 31**
29	156.947	0.7830	227.115	24.9510	7, 10, 14, 37, 34
30	162.495	0.7969	226.774	25.0958	6, 10, 14, 37, 34

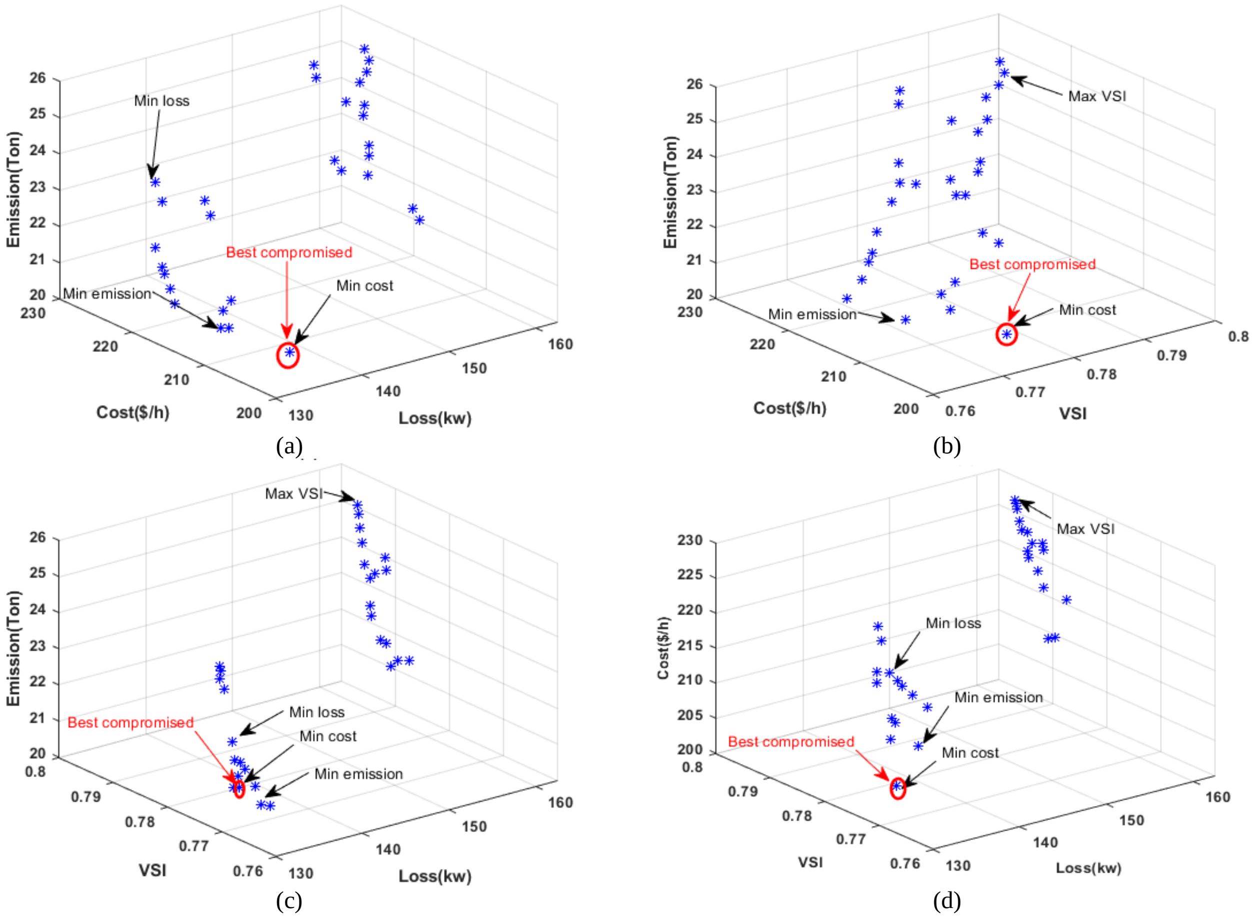

Fig. 13 The Pareto optimal solutions (case study 1).

indicates the three objective functions which are plotted versus each other without taking into consideration the fourth objective function. Given the priority of MGO, the arrow sign solutions represent the optimal solutions. The red circles in Fig. 14 depicts the best-compromised solution that is solution number 1 in Table 5. It has coordinates (106.908kW (power loss), 161.144$/h (operation cost), 13.229×10^3 tons (emission), 0.7562 (VSI)) that denote a suitable compromise among the objectives.

6.2.3 Case study 3

This case study considers the DFR and generation scheduling of combined energy systems simultaneously. Table 6 denotes the Pareto solutions of the optimal DFR and generation scheduling of the combined energy systems and values of objective functions at each solution. In this case study, the best optimal solution for power loss, VSI are related to solution numbers 12, and 13, respectively, while the solution number 6 has the best solution for operation cost and emission. Nevertheless, the best compromised solution corresponds to solution number 10. Similar to the previous case study, the FCs reduce the output power. Fig. 15 exemplifies the 3D plots of the objective functions.

6.2.4 Comparative Studies

To assess the proposed model and comparison the case studies, a comparative analysis is carried out in this subsection. Regarding the four objective functions proposed by this paper, Table 7 compares the results of case studies with respect to its best-compromised solution. In order to show the efficacy of the proposed algorithm in comparison to another algorithm, the simulation of Case study 3 is repeated by the HBB-BC algorithm proposed by [2]. The last row of the Table 7 displays the results of the HBB-BC algorithm.

Despite the lack of combined energy systems in the Case study 1, the results display that all objective functions of power losses, VSI, operation cost, and emissions are enhanced in comparison to the base case. This is due to the fact that the solving proposed MOP leads to the determination of the optimal open switches (7, 9, 14, 28, 31) in which all objective functions improve. Again, comparing the results of Case study 2 and Case study 1 shows that utilizing the optimal combined energy systems instead of optimal DFR improves all of the objective functions except the VSI. In Case study 3, all objective functions are enhanced in comparison to the other case studies. These results show that a better solution is obtained, whenever the optimal

Table 5 Set of the Pareto solutions (case study 2).

Solution number	Power losses [kW]	VSI	Cost [$/h]	Emission [tons]	DG power for the best solution [kW]					
					P_1^{WT}	P_1^{FC}	P_1^{PV}	P_2^{WT}	P_2^{FC}	P_2^{PV}
1	**106.908**	**0.7562**	**161.144**	**13.2296**	**311.96**	**0**	**369.05**	**400.00**	**06.38**	**400.00**
2	107.618	0.7568	162.583	13.4391	298.55	0	383.95	369.84	04.59	400.00
3	126.356	0.7644	164.022	14.1671	282.20	19.36	362.45	391.68	00.00	387.83
4	106.712	0.7490	166.657	13.3024	322.00	00.66	357.231	400.00	05.23	400.00
5	126.509	0.7659	163.433	13.9930	283.00	15.96	363.068	388.10	00.00	405.77
6	124.687	0.7633	170.326	14.6167	244.45	06.53	363.170	400.00	92.70	397.01
7	106.731	0.7518	167.189	13.5227	319.13	02.53	356.722	395.36	17.49	400.00
8	108.153	0.7585	162.371	13.6093	353.42	07.40	362.760	341.05	00.00	384.22
9	130.137	0.7786	173.165	15.6811	191.43	12.23	339.826	400.00	161.27	400.00
10	108.964	0.7626	166.146	15.0358	282.20	00.00	258.608	399.36	149.52	400.00
11	127.268	0.7694	169.737	14.2596	269.22	08.13	379.245	400.00	51.58	374.84
12	127.491	0.7709	172.306	15.3614	241.56	20.51	338.187	386.73	102.53	378.86
13	127.801	0.7720	170.269	14.5498	246.06	07.83	374.023	400.00	80.57	386.80
14	106.551	0.7557	168.646	14.1435	294.66	01.21	338.085	394.11	77.89	393.50
15	129.149	0.7762	172.76	15.5709	225.45	14.92	343.204	400.00	143.27	370.20
16	108.675	0.7622	165.151	14.8607	286.30	00.00	273.273	400.00	141.86	405.97
17	125.761	0.7653	173.561	15.7657	182.54	10.86	354.979	396.52	171.10	384.74
18	106.673	0.7535	167.739	13.7441	312.16	04.63	343.297	390.10	28.73	400.00
19	128.125	0.7729	170.693	14.6698	237.50	08.53	368.996	400.00	86.70	390.01
20	108.576	0.7610	170.133	14.7288	292.69	00.36	284.543	400.00	131.77	400.00
21	128.850	0.7743	172.132	15.0515	224.50	10.16	345.457	400.00	107.00	387.21
22	108.828	0.7623	171.253	14.9797	285.88	01.83	267.335	400.00	141.22	400.00
23	130.463	0.7796	173.377	15.8572	186.46	10.11	342.078	400.00	187.96	394.32
24	124.958	0.7596	169.969	14.4514	260.77	10.43	372.385	400.00	62.56	380.82
25	106.223	0.7509	161.897	13.5011	305.34	00.00	347.812	400.00	21.70	408.96
26	128.949	0.7755	172.035	15.2384	226.88	14.71	337.573	400.00	113.64	394.84
27	106.706	0.7544	168.086	13.8395	312.23	02.96	340.337	392.31	42.01	400.00
28	107.711	0.7568	155.651	13.2384	315.51	00.00	368.494	400.00	00.00	398.04
29	125.971	0.7659	174.034	15.9389	172.73	12.33	352.010	396.10	180.04	385.97
30	130.424	0.7801	173.773	16.0313	181.15	11.76	344.126	400.00	197.15	385.05

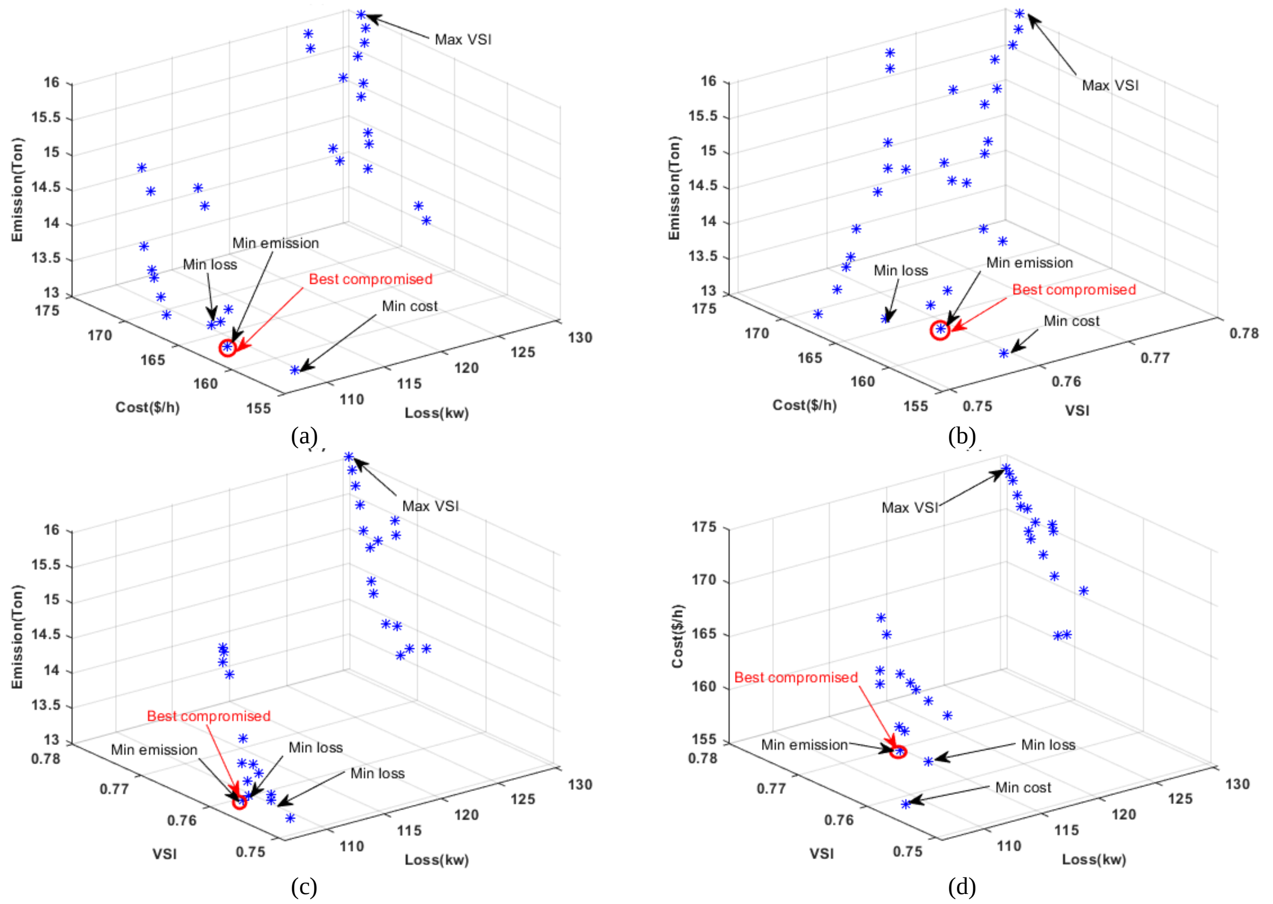

Fig. 14 The Pareto optimal solutions (case study 2).

Table 6 Set of the non-dominated solutions (case study 3).

Solution number	Power losses [kW]	VSI	Cost [$/h]	Emission [tons]	Open switches in the best solution	DG power for the best solution [kW]					
						P_1^{WT}	P_1^{FC}	P_1^{PV}	P_2^{WT}	P_2^{FC}	P_2^{PV}
1	91.206	0.7827	155.222	12.9085	7, 10, 13, 27, 30	309.60	00.00	396.38	375.59	00.00	400.00
2	82.216	0.8508	160.721	12.9222	7, 10, 14, 37, 31	305.81	00.00	383.03	400.00	02.32	393.91
3	99.648	0.8142	155.065	12.8909	33, 10, 13, 28, 34	325.80	00.00	398.31	374.40	00.00	386.20
4	82.100	0.8405	160.906	12.9869	7, 10, 13, 37, 31	307.11	06.61	400.00	400.00	00.00	370.56
5	82.774	0.8538	179.741	18.3720	7, 10, 14, 37, 30	160.82	31.30	200.01	350.32	348.42	377.00
6	126.164	0.7534	155.055	12.8899	33, 10, 13, 28, 15	324.73	00.00	397.09	378.13	00.00	385.11
7	97.465	0.8615	164.669	14.3638	6, 9, 14, 37, 8	234.41	00.00	382.83	358.35	97.93	396.28
8	95.024	0.8519	168.089	13.470	7, 10, 14, 37, 34	300.01	13.01	374.71	373.90	22.71	387.43
9	83.003	0.8513	157.368	13.1476	7, 10, 14, 37, 31	313.21	00.00	394.31	377.41	00.00	353.70
10	**82.758**	**0.8510**	**156.801**	**13.0839**	**7, 10, 14, 37, 31**	**307.23**	**00.00**	**389.30**	**386.60**	**00.00**	**366.90**
11	82.351	0.8523	178.556	18.1202	7, 10, 14, 37, 30	166.30	35.01	216.22	349.08	333.22	384.13
12	81.400	0.8298	173.518	16.0043	7, 10, 14, 37, 30	156.80	36.11	365.39	350.34	183.81	393.42
13	102.906	0.8779	178.379	17.8781	7, 9, 14, 37, 34	167.41	29.02	230.78	345.41	318.06	382.69
14	95.447	0.8532	163.052	13.49362	7, 10, 14, 37, 34	285.20	00.00	373.03	368.38	32.12	399.68
15	97.712	0.8634	170.608	14.5892	6, 9, 14, 37, 8	230.06	04.21	371.91	360.49	111.64	396.69
16	81.407	0.8289	172.783	15.6917	7, 10, 14, 37, 30	179.41	29.81	355.42	365.34	168.13	387.92
17	81.577	0.8223	171.059	14.9459	7, 10, 14, 37, 30	227.44	19.20	357.02	366.11	125.82	389.50
18	101.322	0.8754	177.311	17.4381	7, 10, 14, 37, 34	186.20	32.30	240.81	348.12	284.10	382.79
19	81.660	0.8203	170.343	14.6441	7, 10, 14, 37, 30	242.10	15.44	359.20	369.31	108.47	390.90
20	82.036	0.8414	166.492	13.0046	7, 10, 13, 37, 31	305.32	06.00	397.60	400.00	02.23	374.13
21	102.415	0.8776	178.036	17.738	7, 10, 14, 37, 34	174.61	31.72	226.11	351.13	305.62	384.67
22	84.485	0.8589	174.773	15.3938	6, 9, 14, 37, 31	233.90	07.91	284.20	361.48	140.32	385.13
23	96.451	0.8601	170.833	14.6794	7, 10, 14, 37, 34	235.62	16.18	361.73	374.59	105.84	380.50
24	95.731	0.8571	169.020	13.9865	7, 10, 14, 37, 34	268.81	07.16	372.92	364.62	67.91	397.82
25	83.814	0.8553	165.277	14.4491	6, 9, 14, 37, 31	236.33	00.00	357.90	367.37	99.69	397.65
26	81.991	0.8440	167.080	13.1868	7, 10, 13, 37, 31	299.00	04.33	385.11	397.88	15.00	379.62
27	100.992	0.8746	176.968	17.3097	7, 10, 14, 37, 34	188.40	36.00	244.09	351.55	271.83	383.62
28	84.637	0.8581	174.655	15.1821	6, 9, 14, 37, 31	235.30	04.53	280.36	366.41	124.71	391.30
29	81.631	0.8256	171.941	15.1586	7, 10, 14, 37, 30	198.21	12.73	362.00	363.10	143.20	395.42
30	81.450	0.8315	174.283	16.2738	7, 10, 14, 37, 30	142.50	36.31	365.42	352.48	201.22	384.56

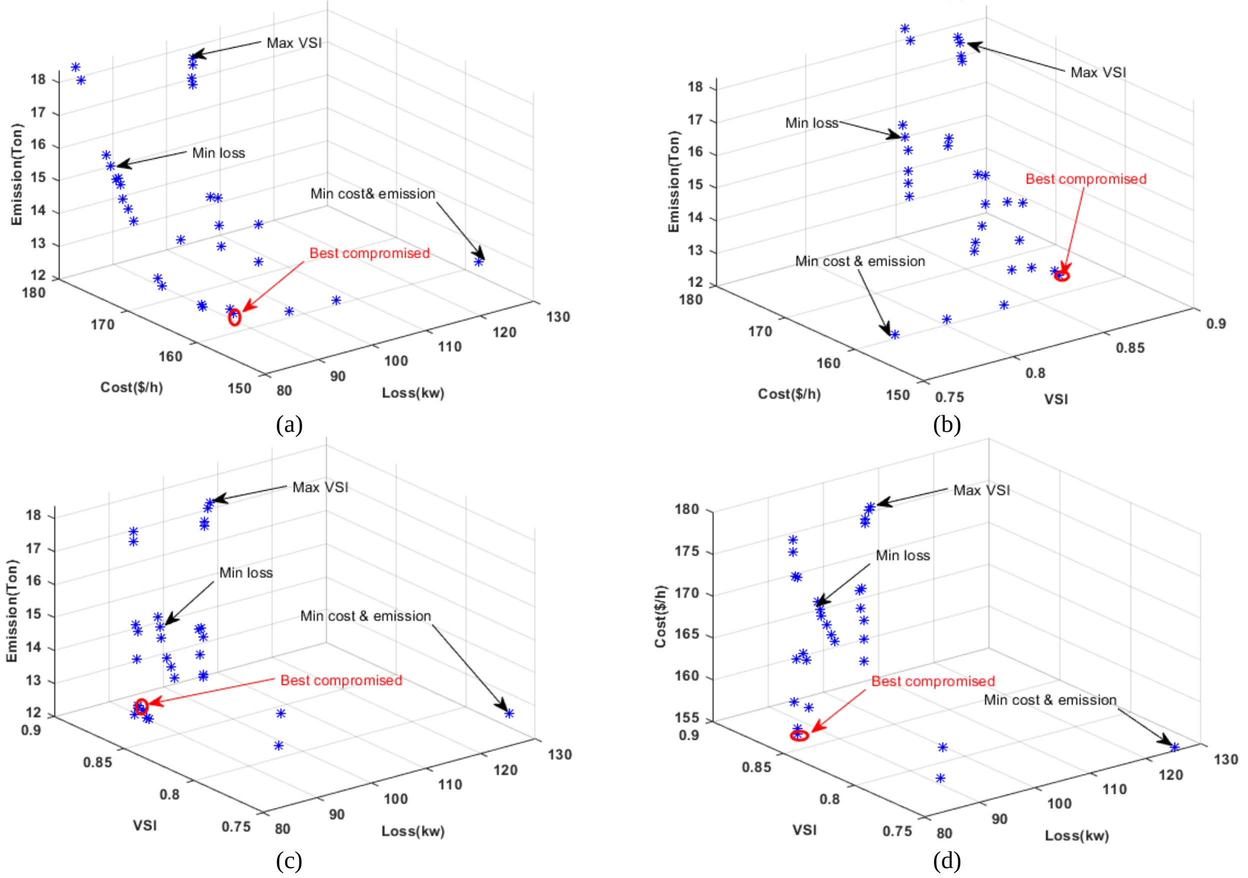

Fig. 15 The Pareto optimal solutions (case study 3).

Table 7 The comparison of the best compromised solutions for different case studies.

Case studies	Power losses [kW]	VSI	Cost [$/h]	Emission [tons]	Minimum voltage [pu]	Open switches in the best solution	DG power for the best solution [kW]					
							P_1^{WT}	P_1^{FC}	P_1^{PV}	P_2^{WT}	P_2^{FC}	P_2^{PV}
Base case	202.67	0.6969	219.38	22.272	0.9131	33, 34, 35, 36, 37	00.00	00.00	00.00	00.00	00.00	00.00
Case study 1	134.197	0.7736	203.124	20.7237	0.9454	7, 9, 14, 37, 31	00.00	00.00	00.00	00.00	00.00	00.00
Case study 2	106.908	0.7562	161.144	13.2296	0.9378	33, 34, 35, 36, 37	311.96	00.00	369.05	400.00	06.38	400.00
Case study 3	82.758	0.8510	156.801	13.0839	0.9489	7, 10, 14, 37, 31	307.23	00.00	389.30	386.60	00.00	366.90
Case study 3 (HBB-BC) [2]	83.456	0.8453	157.768	13.1834	0.9421	7, 10, 14, 37, 31	304.23	00.00	387.34	383.24	00.00	264.34

energy management of the combined energy systems and optimal DFR are simultaneously carried out (as the proposed method), the highest enhancement in objective functions is acquired. The values achieved in Case study 3 for objective functions of power losses (82.75kW), VSI (0.8510), operation cost (156.801$/h), and emissions (13.08 tons) are the most optimal value of all case studies and base case. Regarding the last row of the Table 7, it is seen that although the HBB-BC algorithm has found the status of tie switches similar to proposed algorithm, however, due to fewer use of generations of renewable energies (WT, and PV), the objective functions are converged to unsuitable values compared to the results of the proposed algorithm in Case study 3.

As observed in Table 7, the last case study has also a better minimum voltage. To accurately observe resulted voltage status of MG, voltage profile for all case studies is illustrated by Fig. 16.

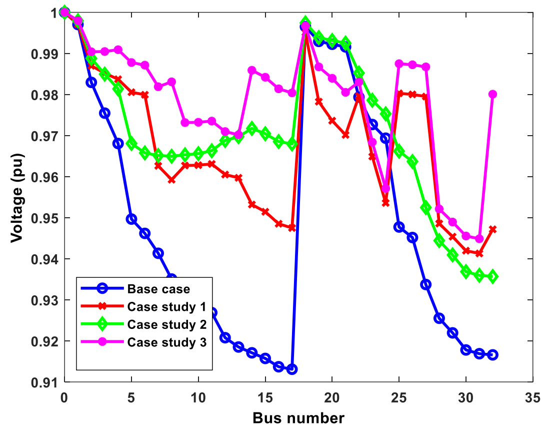

Fig. 16 The voltage profile for all case studies.

It is seen that Case study 2 results in a higher voltage for a number of buses in comparison to the proposed formulation of Case study 3. Yet, Case study 3 improves the weakest bus voltage as motivated by VSI. It can be noted that the voltage instability and voltage collapse of an MG can be triggered by the weakest bus voltage, and subsequently, the reinforcement of the weakest voltage leads to the improvement of the whole power system voltage status. This fact occurs in the proposed MOP where the minimum voltage of 0.9489 p.u. (at bus 31) is higher than other minimum voltages given by other case studies. It is important to also note that the voltage of bus 0 of the MG, which is connected to the upstream main grid, is kept at 1 (p.u.) as observed in Fig. 16. The voltage of combined energy systems connected to buses (4 and 14) cannot be fixed at 1 p.u. due to operating them with unity power factor.

7 Conclusions

In this paper, the optimal DFR, and optimal generation scheduling of combined energy systems are simultaneously carried out by a combined algorithm named IMOPSO algorithm in an MG. Minimization of active power loss, VSI index, operational costs, and emissions are the objective functions. This MOP is optimized by the above-mentioned algorithm considering the uncertainties of WT generation, PV generation, and electrical demand. This paper proposes the copula-based stochastic energy management for the MG. The scenarios are generated by the scenario tree algorithm and scenario reduction is carried out by a clustering algorithm based on the genetic algorithm. To consider all of the probable solutions, a new index named ASO is proposed to aggregate the solutions.

The main achievements of the proposed MOP model as follows:

- The active power loss is reduced by 59.41%, 47.52%, and 33.66% in Case study 3, 2, and 1, respectively compared to the base case.
- The VSI index is increased by 23.18%, 8.63%, and 11.59% in Case study 3, 2, and 1, respectively in comparison to the base case.
- The total operational costs are elucidated by 28.76%, 26.48% and 7.32% in Case study 3, 2, and 1, respectively in comparison to the base case.
- The emissions are reduced by 41.23%, 40.60%, and 9.09% in Case study 3, 2, and 1, respectively in comparison to the base case.

To improve the research work presented in this paper, the following future works can be considered as follows:

- Presenting an optimal day-ahead scheduling and DFR considering uncertainties modeled by copula method.
- Applying the proposed model on unbalanced MGs.

References

[1] I. Ben Hamida, S. B. Salah, F. Msahli, and M. F. Mimouni, "Optimal network reconfiguration and renewable DG integration considering time sequence variation in load and DGs," *Renewable Energy*, Vol. 121, pp. 66–80, 2018.

[2] M. Esmaeili, M. Sedighizadeh, and M. Esmaili, "Multi-objective optimal reconfiguration and DG (distributed generation) power allocation in distribution networks using Big Bang-Big Crunch algorithm considering load uncertainty," *Energy*, Vol. 103, pp. 86–99, 2016.

[3] M. Sedighizadeh, M. Esmaili, and M. Esmaeili, "Application of the hybrid Big Bang-Big Crunch algorithm to optimal reconfiguration and distributed generation power allocation in distribution systems," *Energy*, Vol. 76, pp. 920–930, 2014.

[4] J. C. Leite, I. P. Abril, and M. S. S. Azevedo, "Capacitor and passive filter placement in distribution systems by nondominated sorting genetic algorithm-II," *Electric Power Systems Research*, Vol. 143, pp. 482–489, 2017.

[5] M. Sedighizadeh, G. Shaghaghi-Shahr, M. Esmaili, and M. R. Aghamohammadi, "Optimal distribution feeder reconfiguration and generation scheduling for microgrid day-ahead operation in the presence of electric vehicles considering uncertainties," *Journal of Energy Storage*, Vol. 21, pp. 58–71, 2019.

[6] R. Jabbari-Sabet, S. M. Moghaddas-Tafreshi, and S. S. Mirhoseini, "Microgrid operation and management using probabilistic reconfiguration and unit commitment," *International Journal of Electrical Power & Energy Systems*, Vol. 75, pp. 328–336, 2016.

[7] G. Gutiérrez-Alcaraz, E. Galván, N. González-Cabrera, and M. Javadi, "Renewable energy resources short-term scheduling and dynamic network reconfiguration for sustainable energy consumption," *Renewable and Sustainable Energy Reviews*, Vol. 52, pp. 256–264, 2015.

[8] M. Sedighizadeh, "Optimal reconfiguration and capacitor allocation in radial distribution systems using the hybrid shuffled frog leaping algorithm in the fuzzy framework," *Journal of Operation and Automation in Power Engineering*, Vol. 3, No. 1, pp. 56–70, 2015.

[9] F. S. Gazijahani and J. Salehi, "Integrated DR and reconfiguration scheduling for optimal operation of microgrids using Hong's point estimate method," *International Journal of Electrical Power & Energy Systems*, Vol. 99, pp. 481–492, 2018.

[10] M. R. Kaveh, R. A. Hooshmand, and S. M. Madani, "Simultaneous optimization of re-phasing, reconfiguration and DG placement in distribution networks using BF-SD algorithm," *Applied Soft Computing*, Vol. 62, pp. 1044–1055, 2018.

[11] J. Shukla, B. Das, and V. Pant, "Stability constrained optimal distribution system reconfiguration considering uncertainties in correlated loads and distributed generations," *International Journal of Electrical Power & Energy Systems*, Vol. 99, pp. 121–133, 2018.

[12] E. Kianmehr, S. Nikkhah, and A. Rabiee, "Multi-objective stochastic model for joint optimal allocation of DG units and network reconfiguration from DG owner's and DisCo's perspectives," *Renewable Energy*, Vol. 132, pp. 471–485, 2019.

[13] T. T. Nguyen, A. V. Truong, and T. A. Phung, "A novel method based on adaptive cuckoo search for optimal network reconfiguration and distributed generation allocation in distribution network," *International Journal of Electrical Power & Energy Systems*, Vol. 78, pp. 801–815, 2016.

[14] S. Zhang, H. Cheng, D. Wang, L. Zhang, F. Li, and L. Yao, "Distributed generation planning in active distribution network considering demand side management and network reconfiguration," *Applied Energy*, Vol. 228, pp. 1921–1936, 2018.

[15] N. Kanwar, N. Gupta, K. R. Niazi, and A. Swarnkar, "An integrated approach for distributed resource allocation and network reconfiguration considering load diversity among customers," *Sustainable Energy, Grids and Networks*, Vol. 7, pp. 37–46, 2016.

[16] A. Zidan, M. F. Shaaban, and E. F. El-Saadany, "Long-term multi-objective distribution network planning by DG allocation and feeders' reconfiguration," *Electric Power Systems Research*, Vol. 105, pp. 95–104, 2013.

[17] R. S. Rao, K. Ravindra, K. Satish, and S. Narasimham, "Power loss minimization in distribution system using network reconfiguration in the presence of distributed generation," *IEEE Transactions on Power Systems*, Vol. 28, No. 1, pp. 317–325, 2013.

[18] K. Muthukumar and S. Jayalalitha, "Integrated approach of network reconfiguration with distributed generation and shunt capacitors placement for power loss minimization in radial distribution networks," *Applied Soft Computing*, Vol. 52, pp. 1262–1284, 2017.

[19] M. Mohammadi, A. M. Rozbahani, and S. Bahmanyar, "Power loss reduction of distribution systems using BFO based optimal reconfiguration along with DG and shunt capacitor placement simultaneously in fuzzy framework," *Journal of Central South University*, Vol. 24, No. 1, pp. 90–103, 2017.

[20] S. N. Ravadanegh, M. R. J. Oskuee, and M. Karimi, “Multi-objective planning model for simultaneous reconfiguration of power distribution network and allocation of renewable energy resources and capacitors with considering uncertainties,” *Journal of Central South University*, Vol. 24, No. 8, pp. 1837–1849, 2017.

[21] M. Sedighizadeh, M. Dakhem, M. Sarvi, and H. H. Kordkheili, “Optimal reconfiguration and capacitor placement for power loss reduction of distribution system using improved binary particle swarm optimization,” *International Journal of Energy and Environmental Engineering*, Vol. 5, No. 1, p. 3, 2014.

[22] H. Nasiraghdam and S. Jadid, “Optimal hybrid PV/WT/FC sizing and distribution system reconfiguration using multi-objective artificial bee colony (MOABC) algorithm,” *Solar Energy*, Vol. 86, No. 10, pp. 3057–3071, 2012.

[23] T. Niknam, A. K. Fard, and A. Seifi, “Distribution feeder reconfiguration considering fuel cell/wind/photovoltaic power plants,” *Renewable Energy*, Vol. 37, No. 1, pp. 213–225, 2012.

[24] J. Olamaei, T. Niknam, and G. Gharehpetian, “Application of particle swarm optimization for distribution feeder reconfiguration considering distributed generators,” A*pplied Mathematics and Computation*, Vol. 201, No. 1–2, pp. 575–586, 2008.

[25] M. Sedighizadeh, S. Ahmadi, and M. Sarvi, “An efficient hybrid big bang–big crunch algorithm for multi-objective reconfiguration of balanced and unbalanced distribution systems in fuzzy framework,” *Electric Power Components and Systems*, Vol. 41, No. 1, pp. 75–99, 2013.

[26] M. Sedighizadeh, M. Ghalambor, and A. Rezazadeh, “Reconfiguration of radial distribution systems with fuzzy multi-objective approach using modified big bang-big crunch algorithm,” *Arabian Journal for Science and Engineering*, Vol. 39, No. 8, pp. 6287–6296, 2014.

[27] M. Sedighizadeh, M. Esmaili, and N. Mohammadkhani, “Stochastic multi-objective energy management in residential microgrids with combined cooling, heating, and power units considering battery energy storage systems and plug-in hybrid electric vehicles,” *Journal of Cleaner Production*, Vol. 195, pp. 301–317, 2018.

[28] E. Shahryari, H. Shayeghi, B. Mohammadi-Ivatloo, and M. Morad Zadeh, “Optimal energy management of microgrid in day-ahead and intra-day markets using a copula-based uncertainty modeling method,” *Journal of Operation and Automation in Power Engineering*, 2019.

[29] S. Hagspiel, A. Papaemannouil, M. Schmid, and G. Andersson, “Copula-based modeling of stochastic wind power in Europe and implications for the Swiss power grid,” *Applied Energy*, Vol. 96, pp. 33–44, 2012.

[30] A. Sklar, A Sklar, and C. A. Sklar, “Fonctions de repartition an dimensions et leurs marges,” *Publ. Inst. Statist. Univ. Paris*, Vol. 8, pp. 229–231, 1959.

[31] A. Zakariazadeh, S. Jadid, and P. Siano, “Smart microgrid energy and reserve scheduling with demand response using stochastic optimization,” *International Journal of Electrical Power & Energy Systems*, Vol. 63, pp. 523–533, 2014.

[32] M. Sedighizadeh, M. Esmaili, A. Jamshidi, and M. H. Ghaderi, “Stochastic multi-objective economic-environmental energy and reserve scheduling of microgrids considering battery energy storage system,” *International Journal of Electrical Power & Energy Systems*, Vol. 106, pp. 1–16, 2019.

[33] S. Talari, M. Yazdaninejad, and M.-R. Haghifam, “Stochastic-based scheduling of the microgrid operation including wind turbines, photovoltaic cells, energy storages and responsive loads,” *IET Generation, Transmission & Distribution*, Vol. 9, No. 12, pp. 1498–1509, 2015.

[34] M. Motevasel and A. R. Seifi, “Expert energy management of a micro-grid considering wind energy uncertainty,” *Energy Conversion and Management*, Vol. 83, pp. 58–72, 2014.

[35] A. Zakariazadeh, S. Jadid, and P. Siano, “Economic-environmental energy and reserve scheduling of smart distribution systems: A multiobjective mathematical programming approach,” *Energy Conversion and Management*, Vol. 78, pp. 151–164, 2014.

[36] M. Petrollese, L. Valverde, D. Cocco, G. Cau, and J. Guerra, “Real-time integration of optimal generation scheduling with MPC for the energy management of a renewable hydrogen-based microgrid,” *Applied Energy*, Vol. 166, pp. 96–106, 2016.

[37] W. Su, J. Wang, and J. Roh, “Stochastic energy scheduling in microgrids with intermittent renewable energy resources,” *IEEE Transactions on Smart Grid*, Vol. 5, no. 4, pp. 1876–1883, 2014.

[38] J. Sachs and O. Sawodny, “Multi-objective three stage design optimization for island microgrids,” *Applied Energy*, Vol. 165, pp. 789–800, 2016.

[39] A. Jose-Garcia and W. Gómez-Flores, “Automatic clustering using nature-inspired metaheuristics: A survey,” *Applied Soft Computing*, Vol. 41, pp. 192–213, 2016.

[40] M. C. Fu, *Handbook of simulation optimization*. Springer New York, 2015.

[41] M. Sedighizadeh and R. Bakhtiary, "Optimal multi-objective reconfiguration and capacitor placement of distribution systems with the Hybrid Big Bang–Big Crunch algorithm in the fuzzy framework," *Ain Shams Engineering Journal*, Vol. 7, No. 1, pp. 113–129, 2016.

[42] C. A. C. Coello, G. T. Pulido, and M. S. Lechuga, "Handling multiple objectives with particle swarm optimization," IE*EE Transactions on Evolutionary Computation*, Vol. 8, No. 3, pp. 256–279, 2004.

[43] N. Al Moubayed, A. Petrovski, and J. McCall, "D2MOPSO: MOPSO based on decomposition and dominance with archiving using crowding distance in objective and solution spaces," *Evolutionary Computation*, Vol. 22, No. 1, pp. 47–77, 2014.

[44] M. Sedighizadeh, A. H. Mohammadpour, and S. M. M. Alavi, "A two-stage optimal energy management by using ADP and HBB-BC algorithms for microgrids with renewable energy sources and storages," *Journal of Energy Storage*, Vol. 21, pp. 460–480, 2019.

[45] N. Zhang, C. Kang, Q. Xia, and J. Liang, "Modeling conditional forecast error for wind power in generation scheduling," *IEEE Transactions on Power Systems*, Vol. 29, No. 3, pp. 1316–1324, 2013.

[46] M. E. Baran and F. F. Wu, "Network reconfiguration in distribution systems for loss reduction and load balancing," *IEEE Transactions on Power Delivery*, Vol. 4, No. 2, pp. 1401–1407, 1989.

M. Khajevand received the B.Sc. degree in Electrical Engineering from the Power and Water University of Technology, Tehran, Iran and M.Sc. degree in Electrical Engineering from Qazvin branch, Islamic Azad university, Qazvin, Iran in 2002 and 2007, respectively. He is currently a Ph.D. Candidate at the faculty of Electrical, Biomedical and Mechatronics Engineering of Islamic Azad University, Qazvin Branch. His research interests are distribution systems, smart grid, electric vehicles and renewable energies.

A. Fakharian received his B.Sc. and M.Sc. degrees in Control Engineering from University of Tehran, Iran in 1999 and 2002. He received his Ph.D. degree in Control Engineering from Tarbiat Modares University, Iran in 2010. Now, he is an Associate Professor at the Faculty of Electrical, Bio-medical and Mechatronics Engineering of Islamic Azad University, Qazvin Branch. His research interests include convex optimization, large scale systems modeling and control, singular perturbation systems control and robust control. He was the recipient of a postdoctoral program award from Lulea University of Technology, Sweden in 2010. Now, he is a guest researcher in this university with some collaborating works in the field of control and optimization of complex and large scale systems especially with application in microgrids and biological systems.

M. Sedighizadeh received the B.Sc. degree in Electrical Engineering from the Shahid Chamran University of Ahvaz, Iran and M.Sc. and Ph.D. degrees in Electrical Engineering from the Iran University of Science and Technology (IUST), Tehran, Iran, in 1996, 1998 and 2004, respectively. From 2000 to 2007 he was with power system studies group of Moshanir Company, Tehran, Iran. Currently, he is as an Associate professor with the Faculty of Electrical Engineering, Shahid Beheshti University, Tehran, Iran. His research interests are Power system control and modeling, FACTS devices, microgrids, and distributed generation.